Electronic Supplementary Material (ESI) for CrystEngComm.

Supporting Information for:

Property Prediction and Pharmacokinetic Evaluation of Mixed Stoichiometry Cocrystals of Zafirlukast, a Drug Delivery Case Study

Philip A. Corner,[a] David J. Berry,[a] James F. McCabe,[b] Rafael Barbas,[c] Rafel Prohens,[c] Hongwen Du,[d] Hongyu Zhou,[d] and Antonio Llinas[e]*

a. Division of Pharmacy, Durham University, Queen's Campus, Stockton on Tees, TS17 6BH, UK.

b. Pharmaceutical Development, AstraZeneca Macclesfield, SK10 2SN, UK.

c. Centres Científics i Tecnològics, Universitat de Barcelona, Spain.

d. PK-BA, Pharmaron, N°6, Tai He road, BDA Beijing, China.

e. Respiratory, Inflammation, Autoimmunity IMED Biotech Unit, AstraZeneca, Gothenburg, Sweden.

E-mail: antonio.llinas@astrazeneca.com

Characterisation of Materials and comparison of batches

Figures S1a-f. Characterisation of powder of **1** zafirlukast.

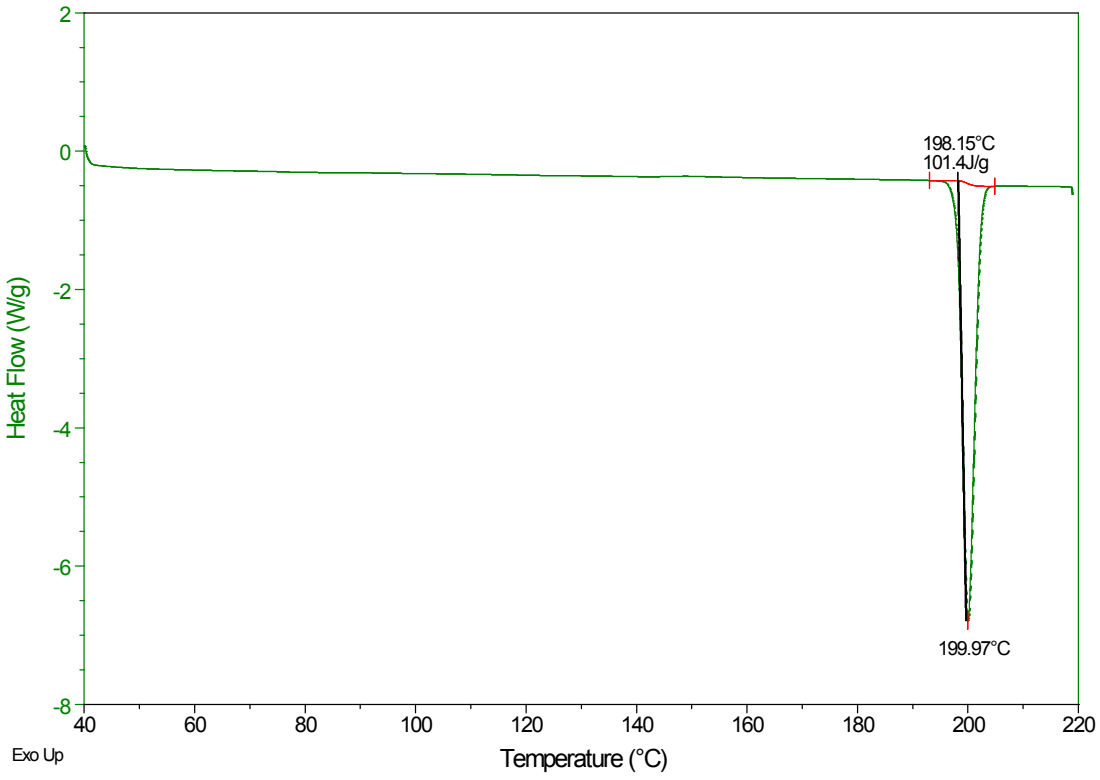

Figure S1a. DSC characterisation of powder of **1** zafirlukast, performed as described in the methods section.

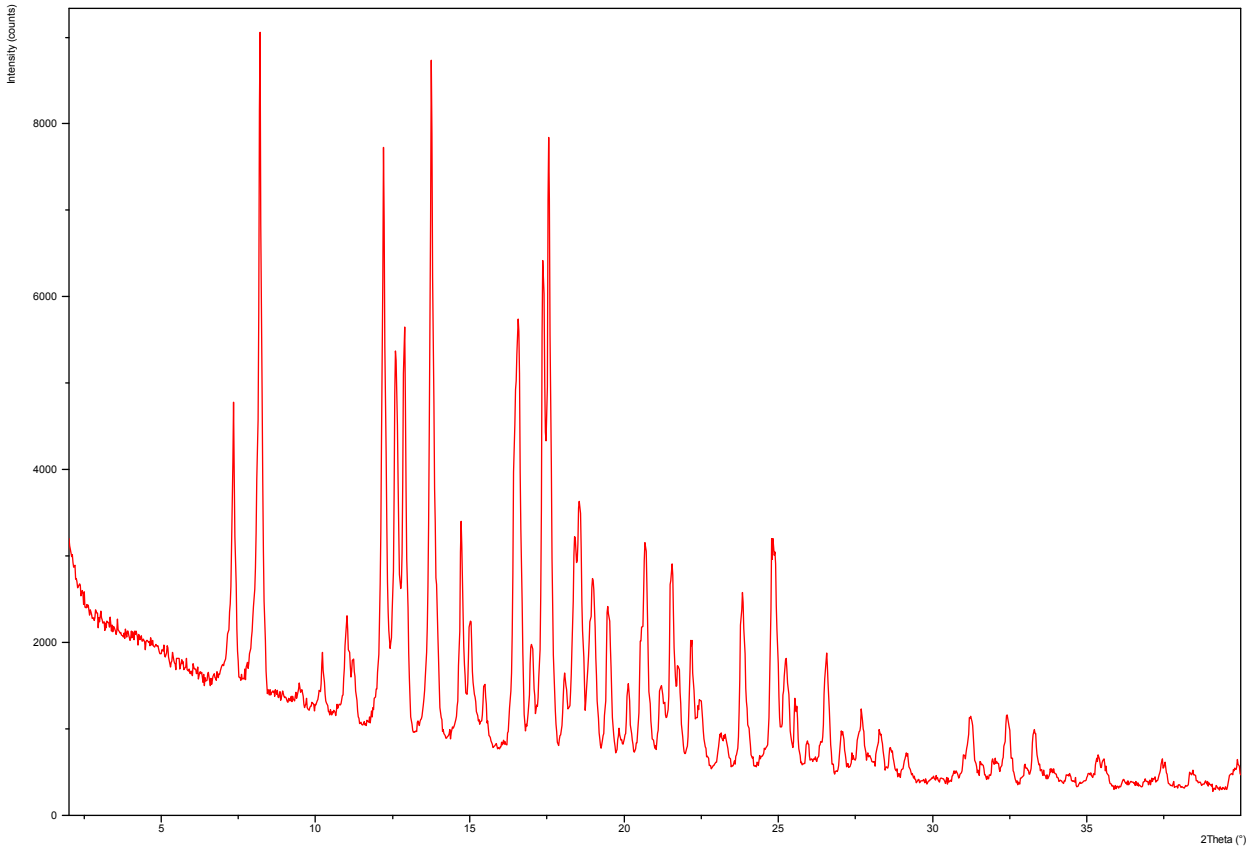

Figure S1b. PXRD characterisation of powder of **1** zafirlukast, performed as described in the methods section.

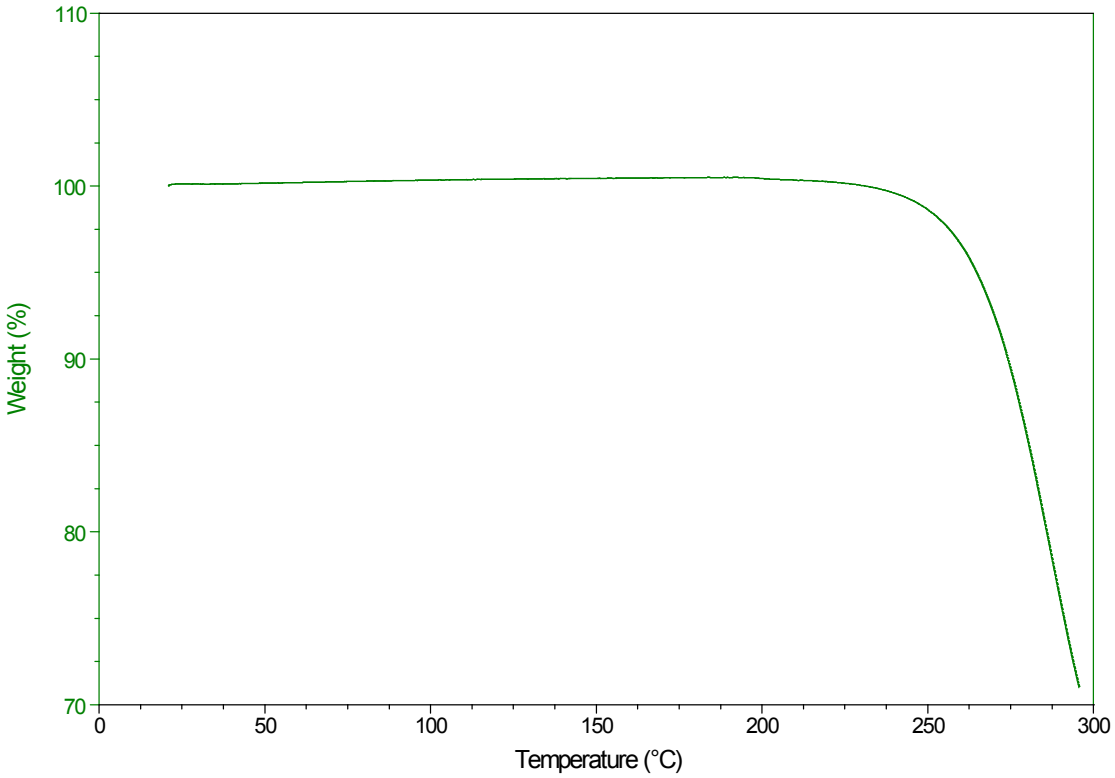

Figure S1c. TGA characterisation of powder of **1** zafirlukast, performed as described in the methods section.

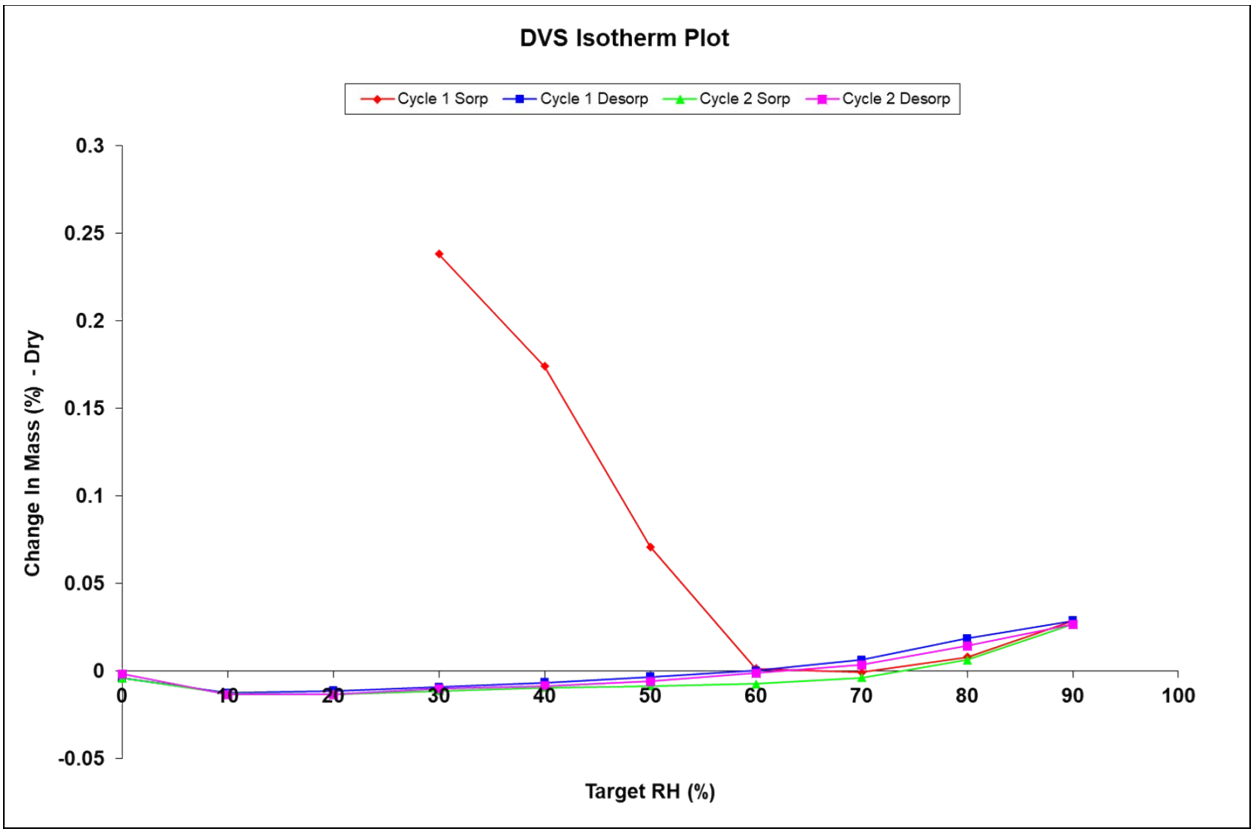

Figure S1d. DVS characterisation of powder of **1** zafirlukast (isotherm plot), performed as described in the methods section.

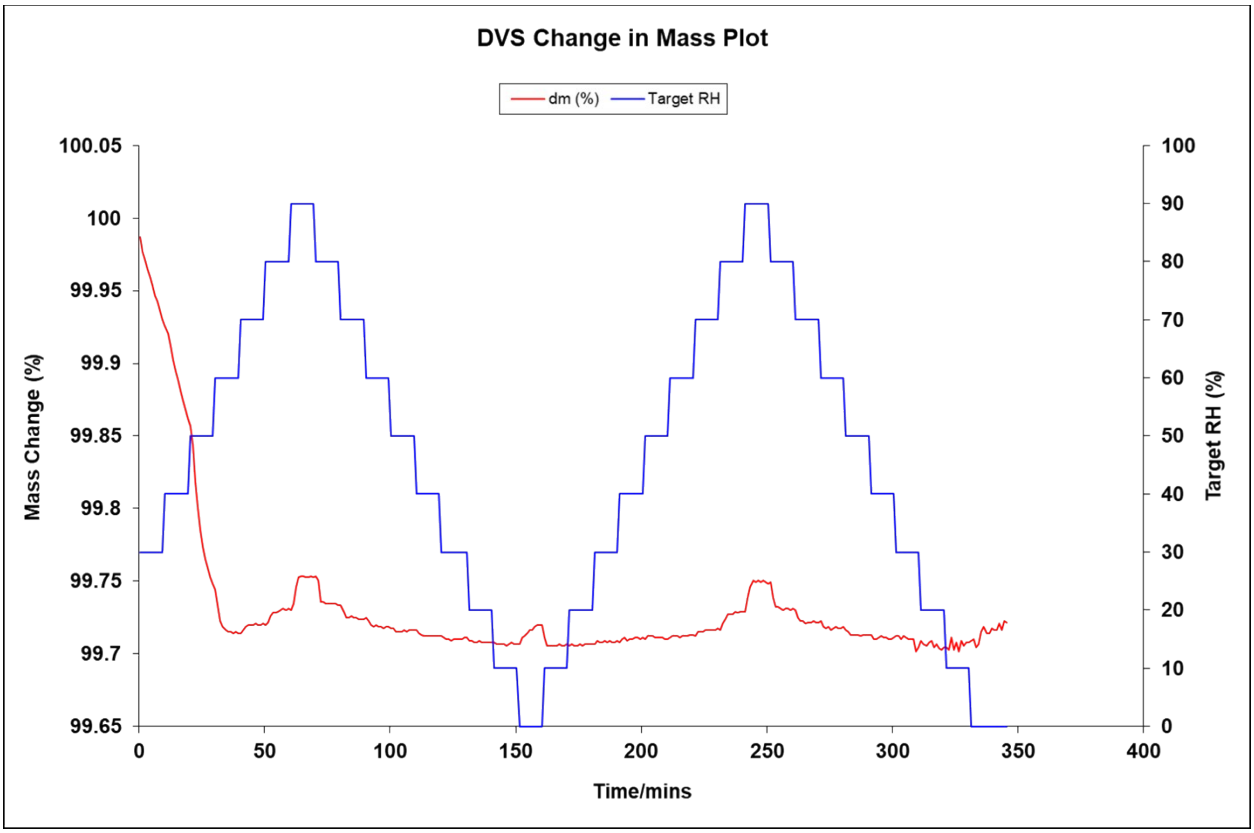

Figure S1e. DVS characterisation of powder of **1** zafirlukast (change in mass plot), performed as described in the methods section.

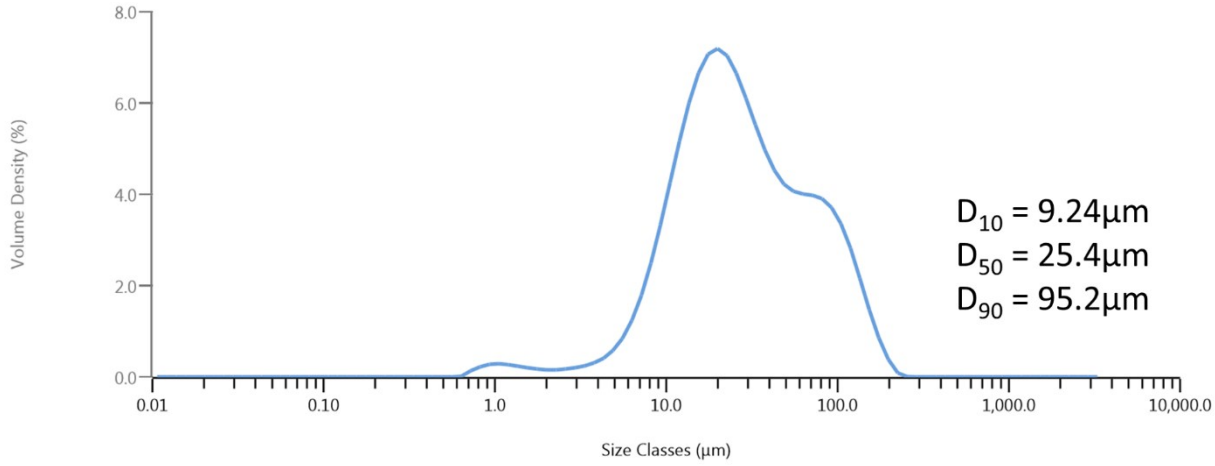

Figure S1f. Particle size determination of powder of **1** zafirlukast, performed as described in the methods section.

Figures S2a-f. Characterisation of powder of **4** zafirlukast:piperazine 1:1 cocrystal.

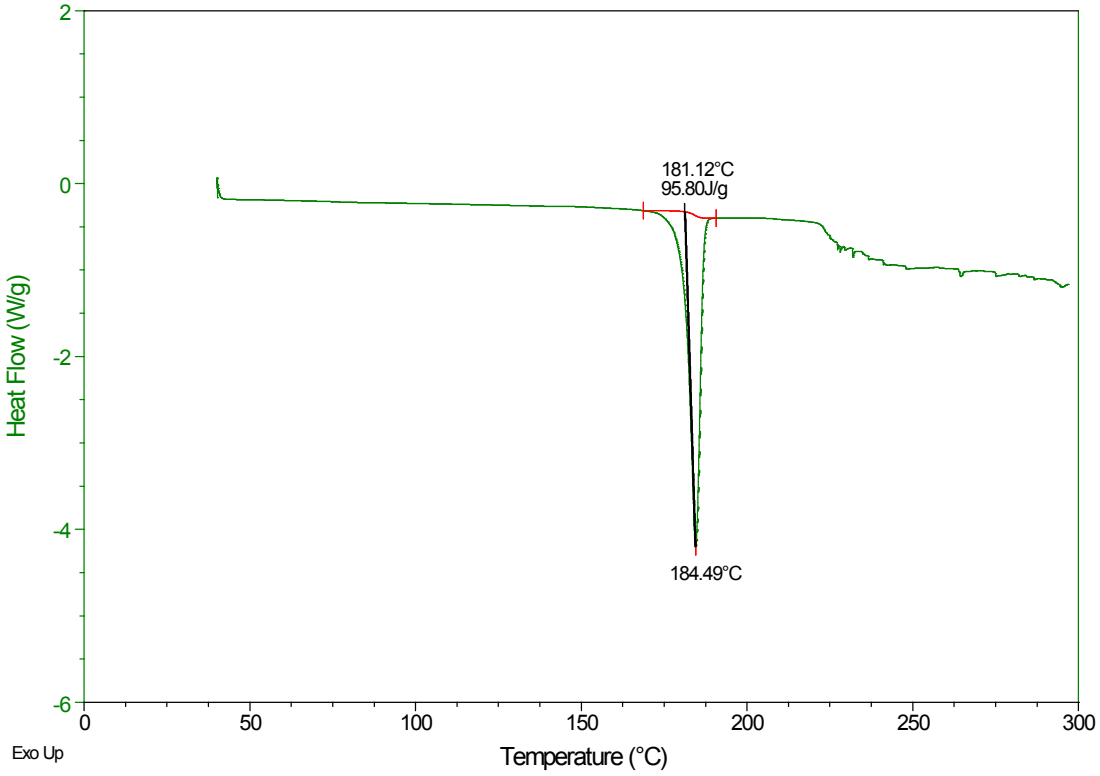

Figure S2a. DSC characterisation of powder of **4** zafirlukast:piperazine 1:1 cocrystal, performed as described in the methods section.

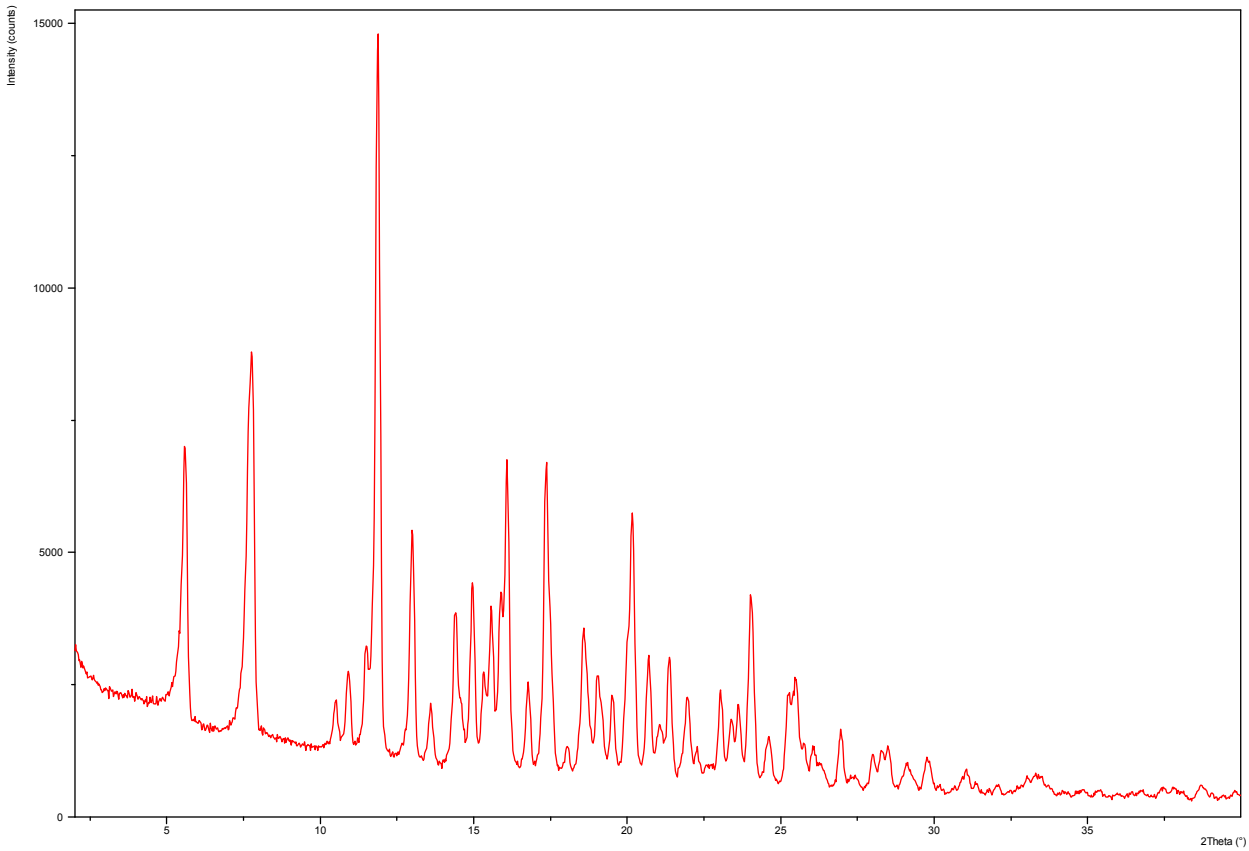

Figure S2b. PXRD characterisation of powder of **4** zafirlukast:piperazine 1:1 cocrystal, performed as described in the methods section.

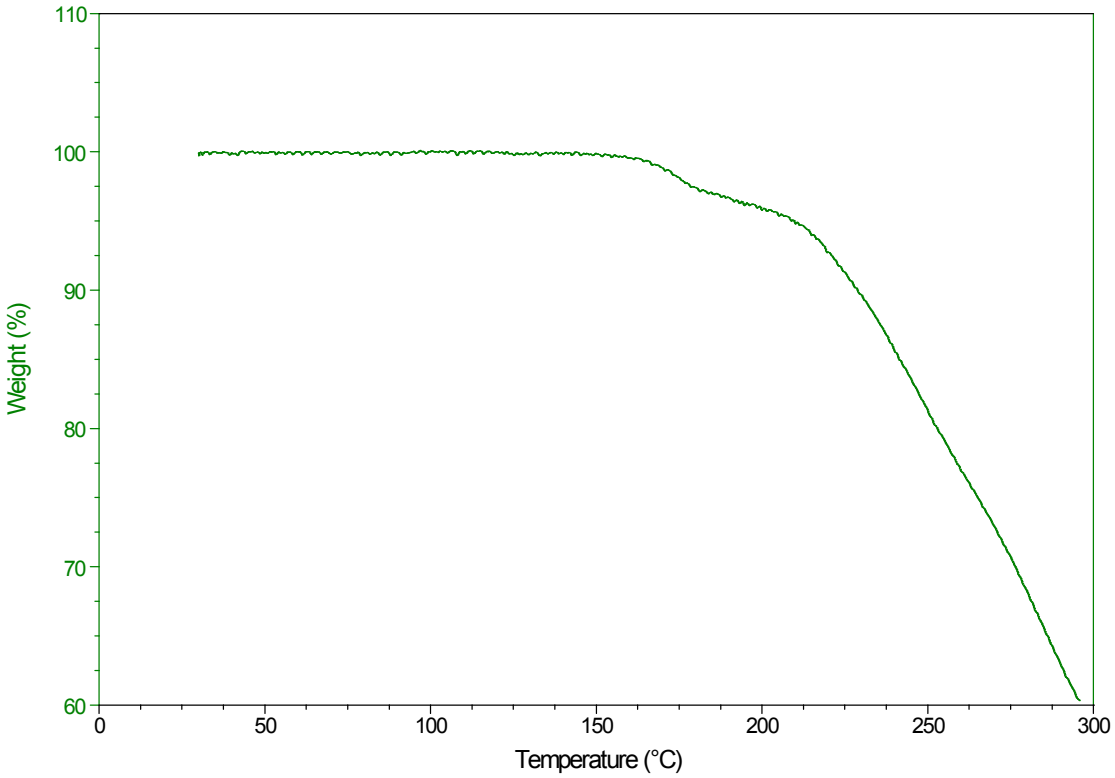

Figure S2c. TGA characterisation of powder of **4** zafirlukast:piperazine 1:1 cocrystal, performed as described in the methods section.

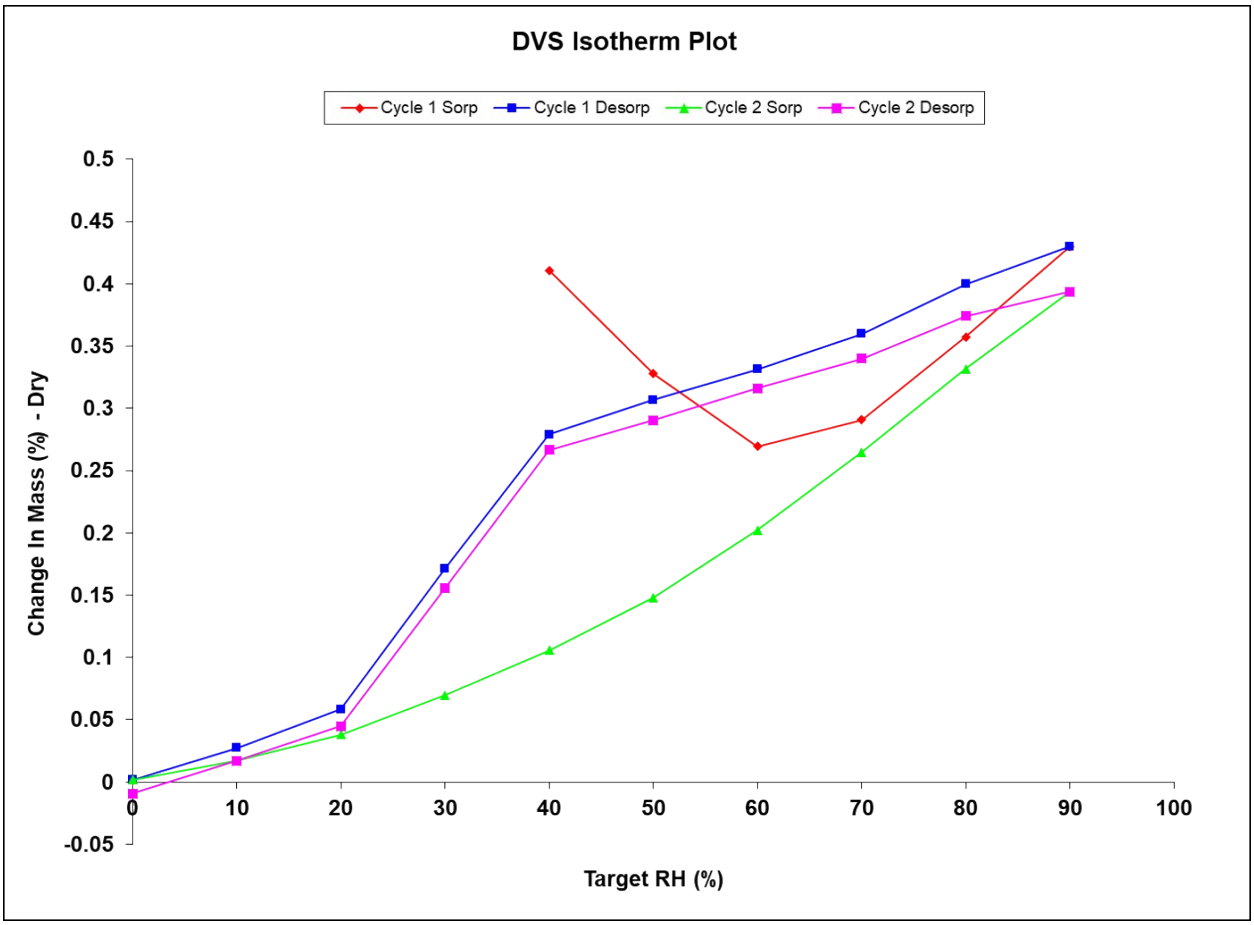

Figure S2d. DVS characterisation of powder of **4** zafirlukast:piperazine 1:1 cocrystal (isotherm plot), performed as described in the methods section.

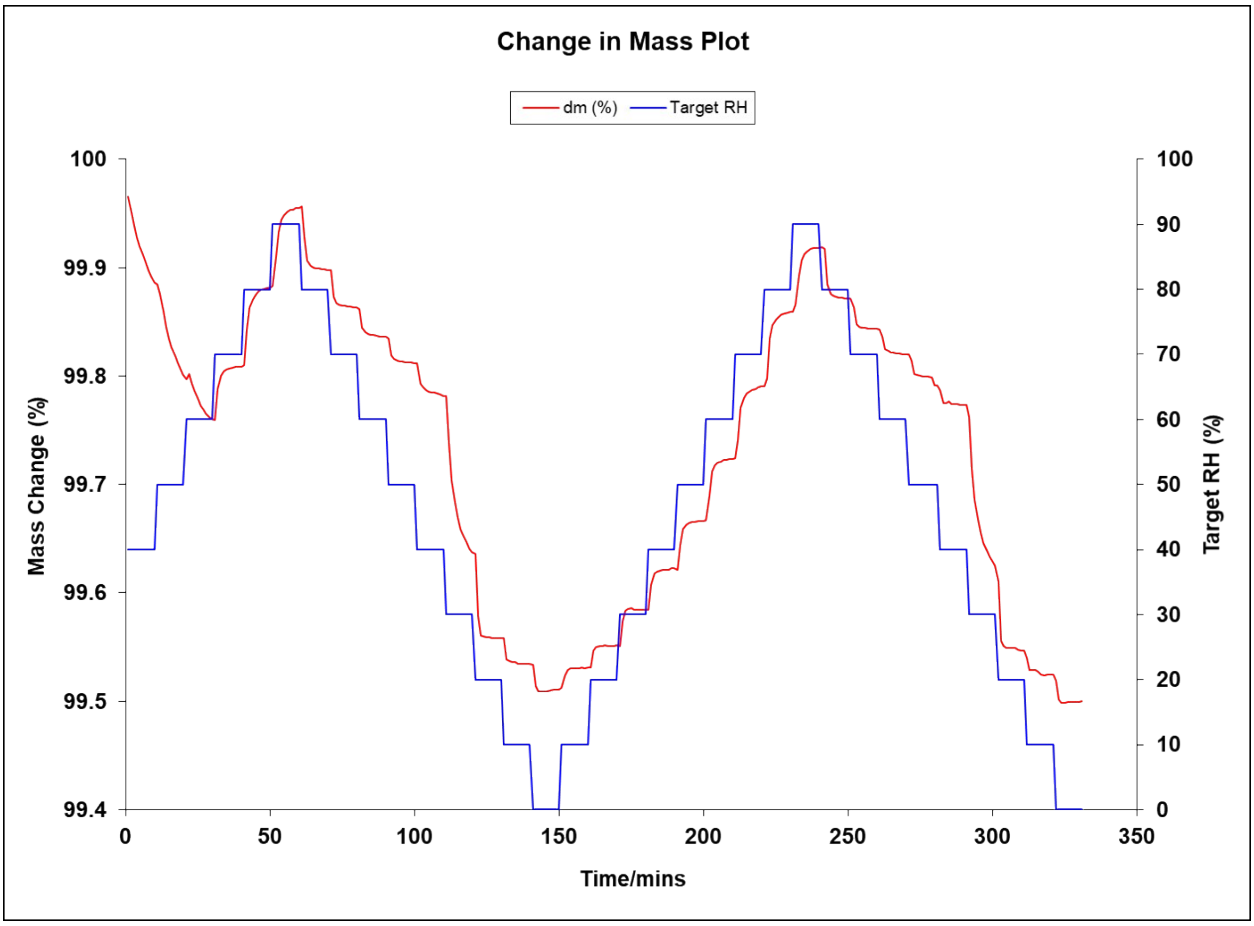

Figure S2e. DVS characterisation of powder of **4** zafirlukast:piperazine 1:1 cocrystal (change in mass plot), performed as described in the methods section.

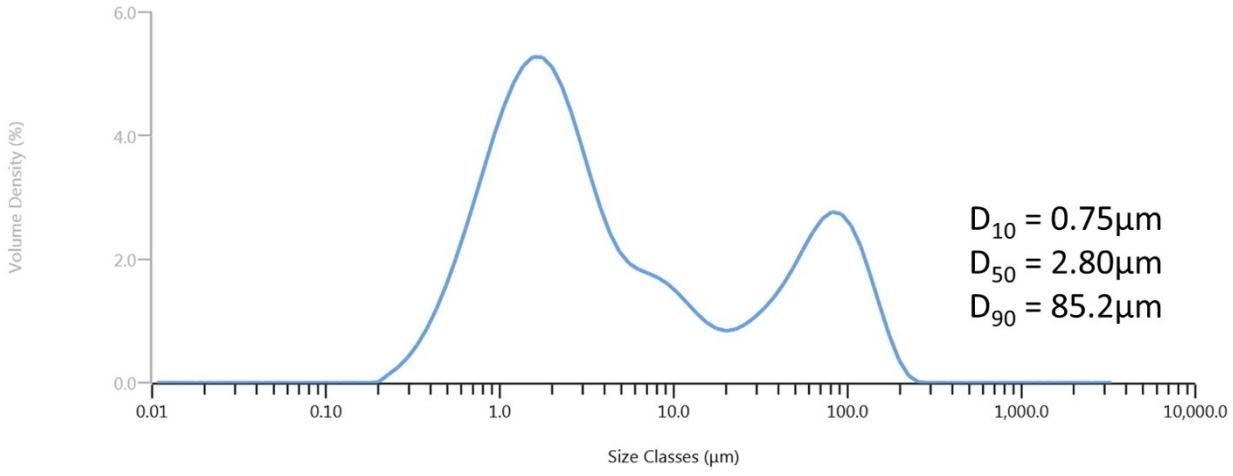

Figure S2f. Particle size determination of powder of **4** zafirlukast:piperazine 1:1 cocrystal, performed as described in the methods section.

Figures S3a-f. Characterisation of powder of **5** zafirlukast:piperazine 2:1 cocrystal.

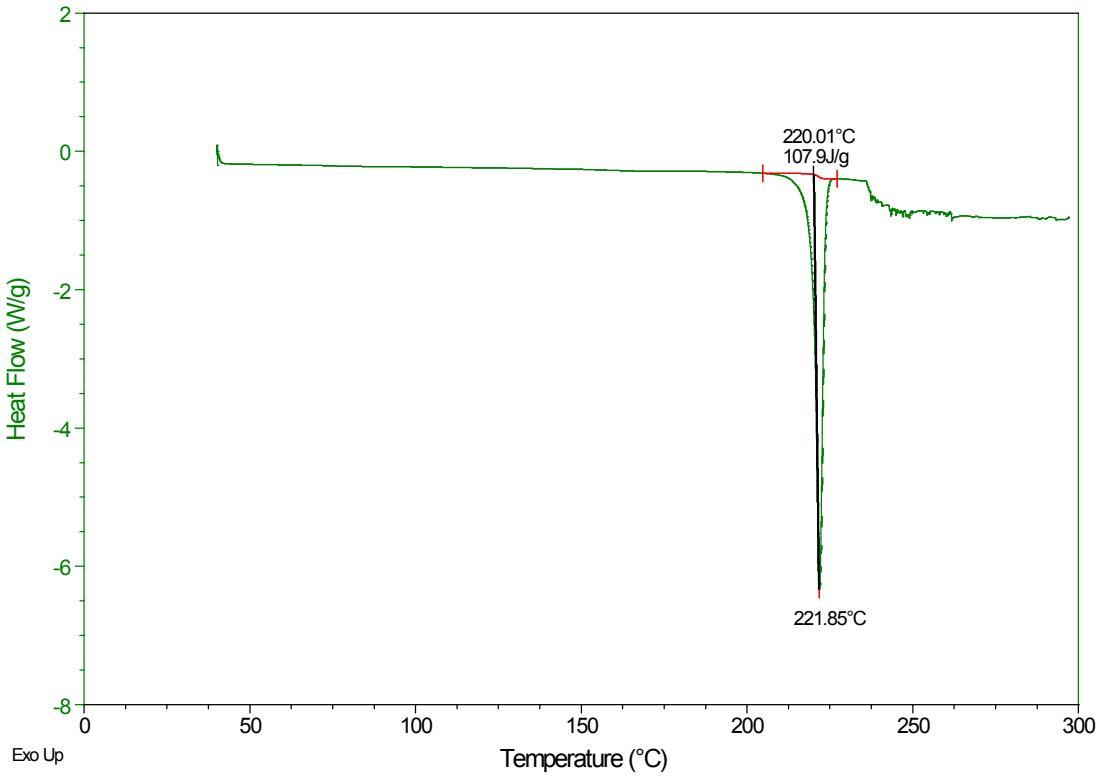

Figure S3a. DSC characterisation of powder of **5** zafirlukast:piperazine 2:1 cocrystal, performed as described in the methods section.

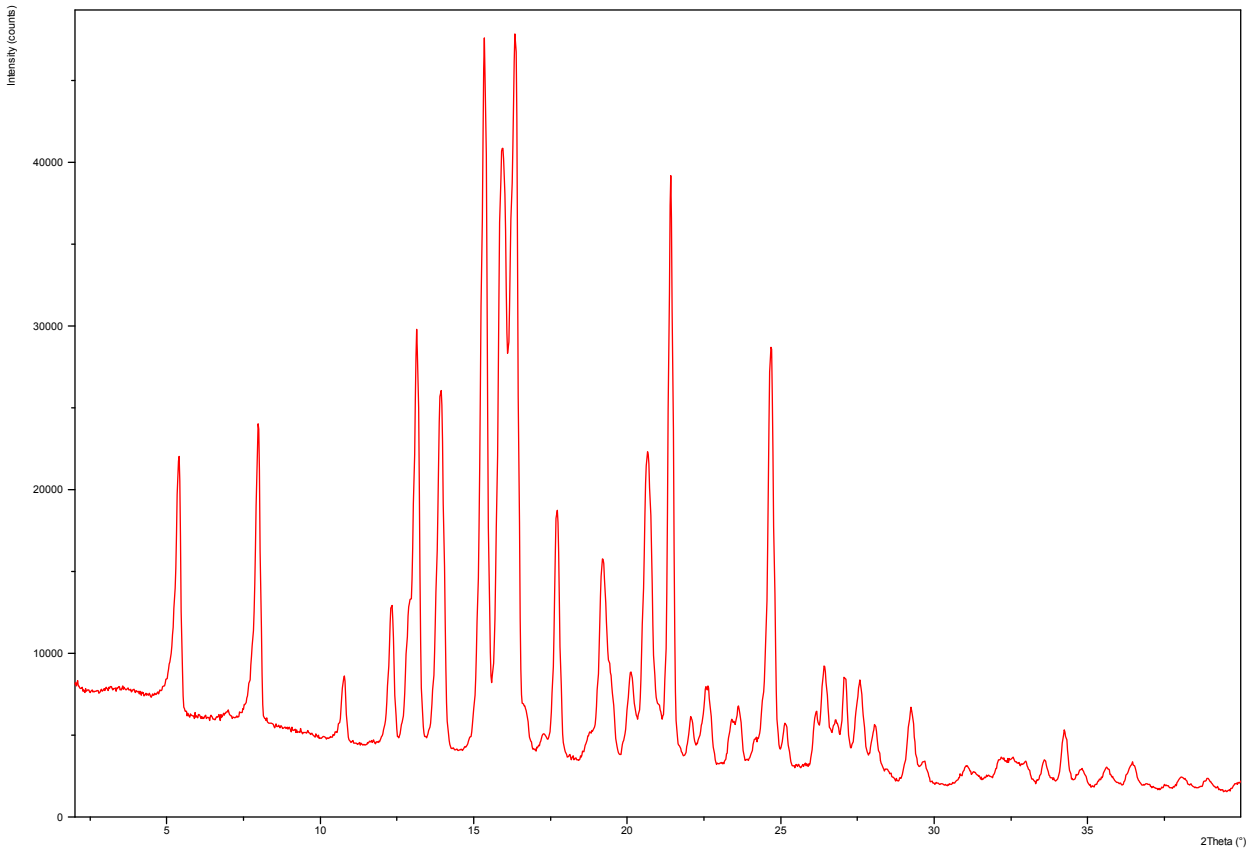

Figure S3b. PXRD characterisation of powder of **5** zafirlukast:piperazine 2:1 cocrystal, performed as described in the methods section.

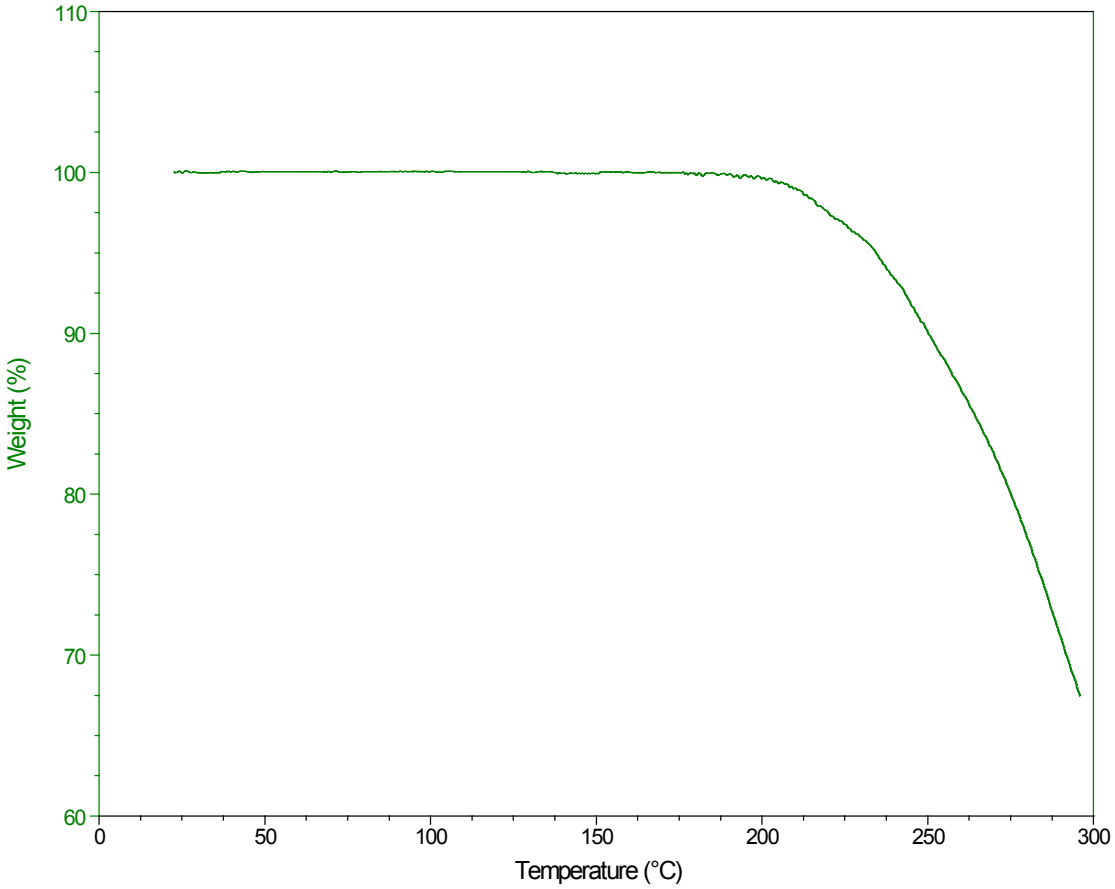

Figure S3c. TGA characterisation of powder of **5** zafirlukast:piperazine 2:1 cocrystal, performed as described in the methods section.

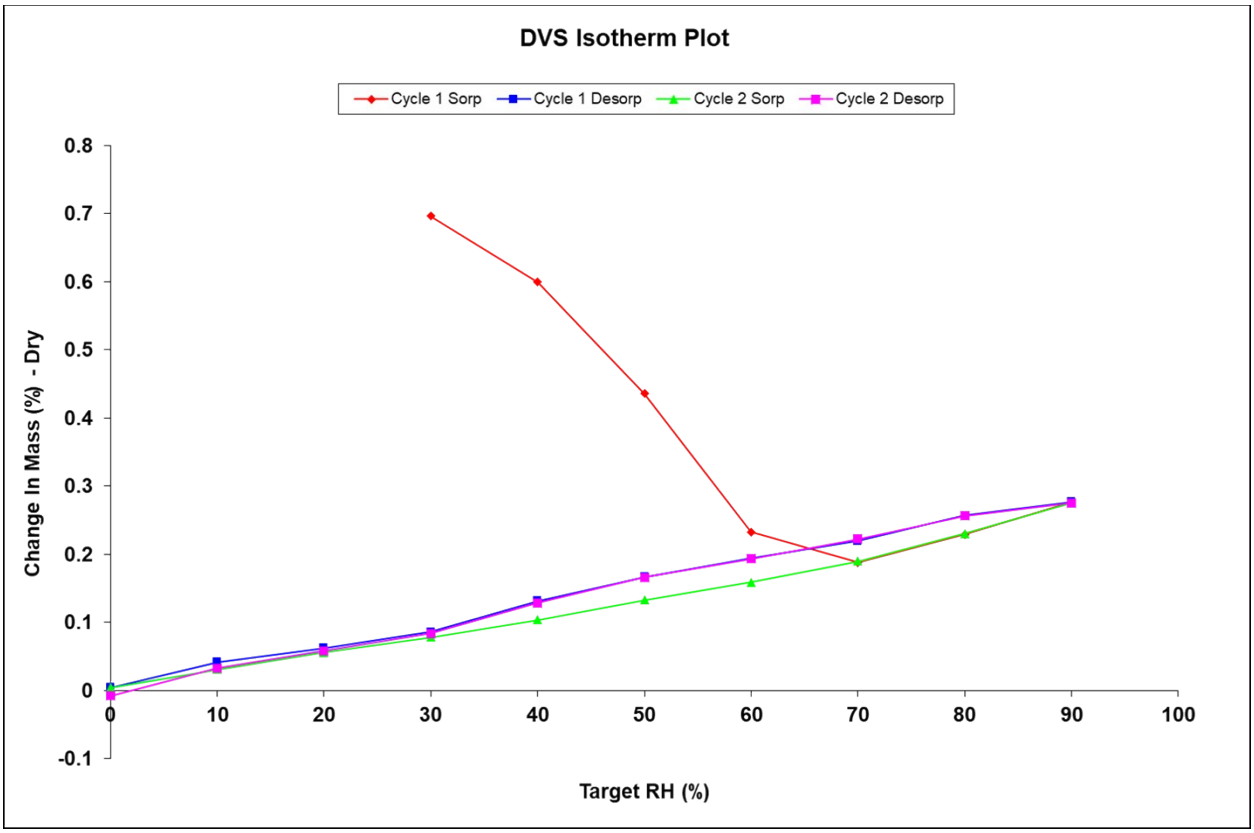

Figure S3d. DVS characterisation of powder of **5** zafirlukast:piperazine 2:1 cocrystal (isotherm plot), performed as described in the methods section.

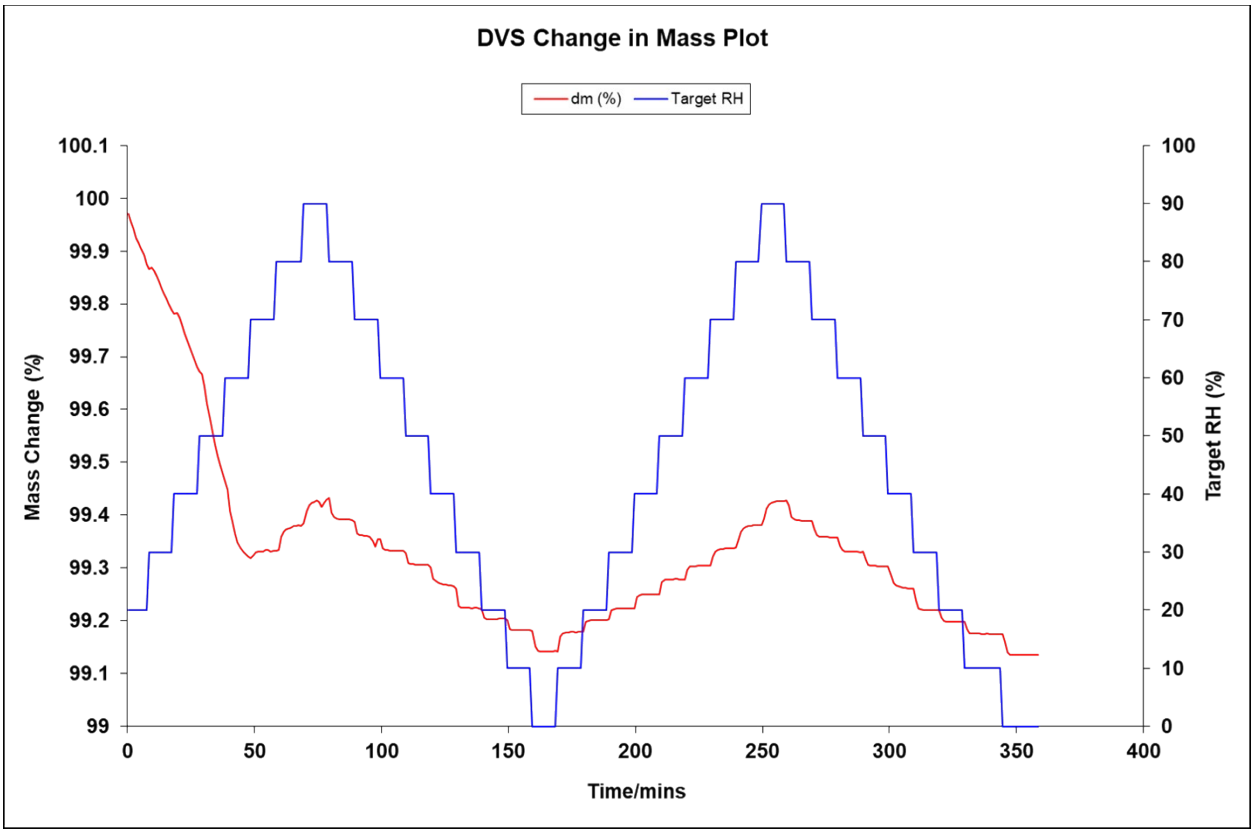

Figure S3e. DVS characterisation of powder of **5** zafirlukast:piperazine 2:1 cocrystal (change in mass plot), performed as described in the methods section.

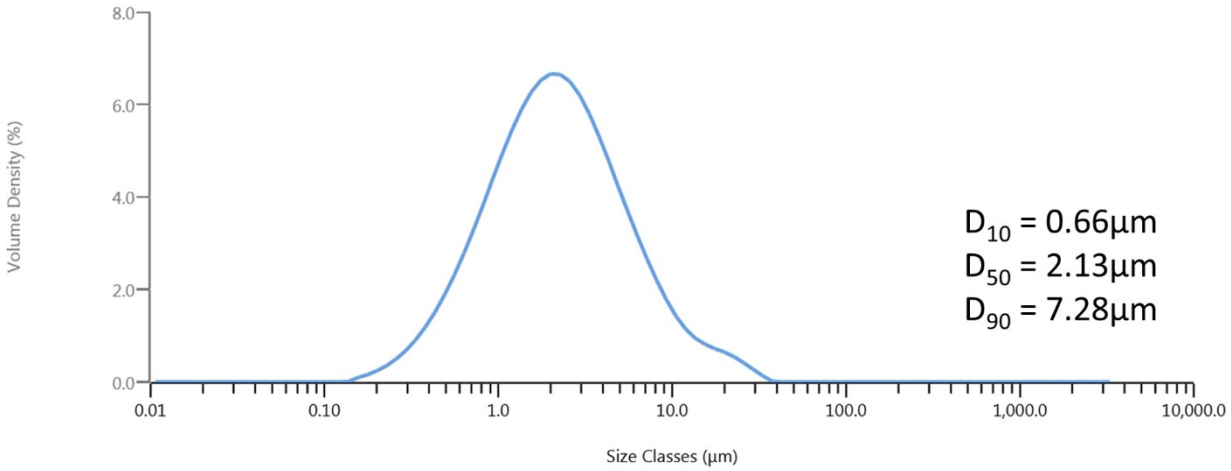

Figure S3f. Particle size determination of powder of **5** zafirlukast:piperazine 2:1 cocrystal, performed as described in the methods section.

Figures S4a-f. Characterisation of powder of **6** zafirlukast:piperazine:toluene 3:3:2 cocrystal.

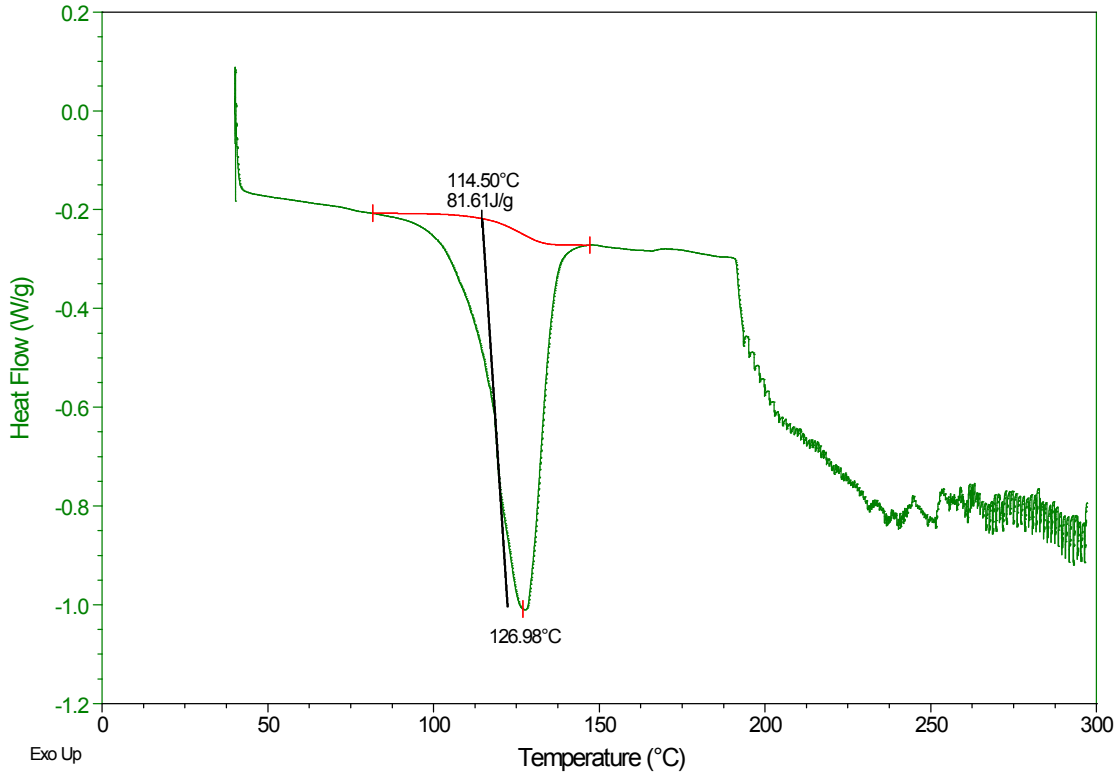

Figure S4a. DSC characterisation of powder of **6** zafirlukast:piperazine:toluene 3:3:2 cocrystal, performed as described in the methods section.

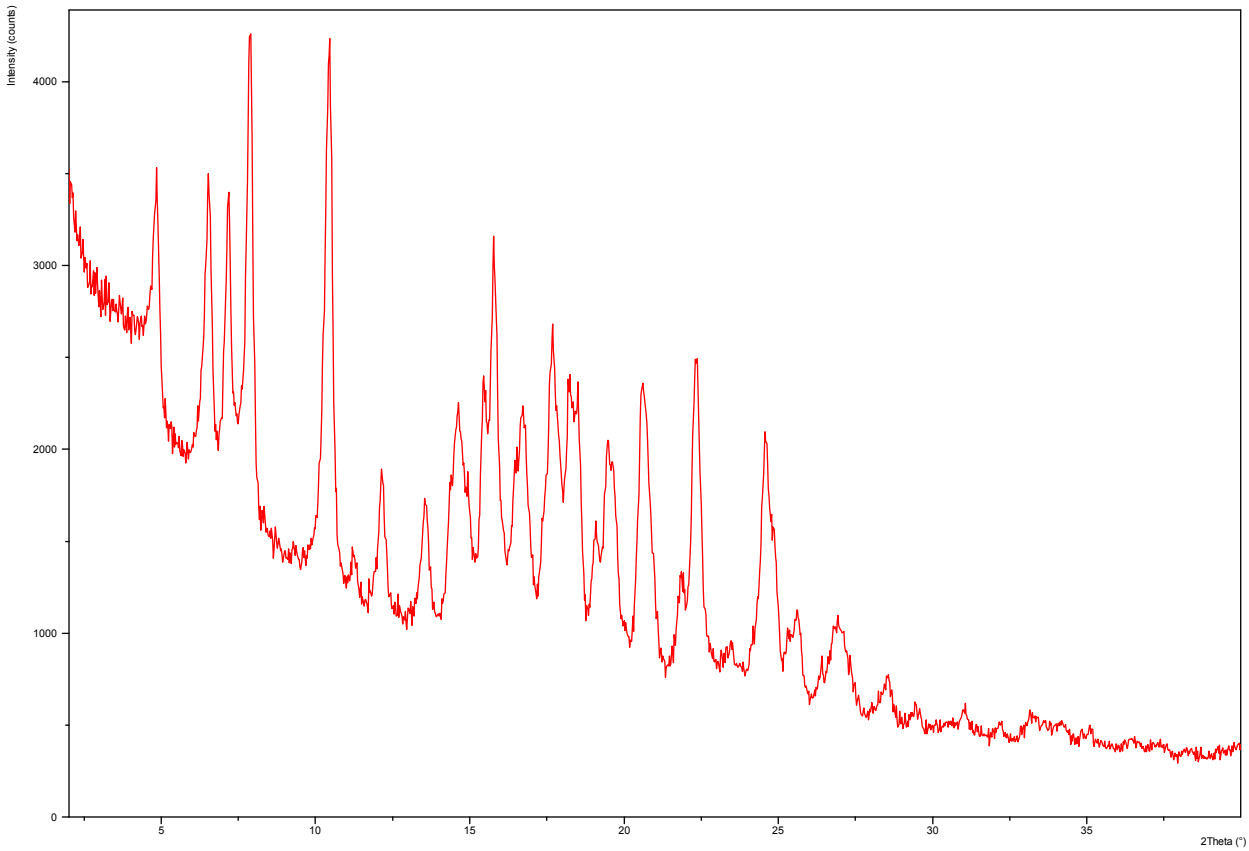

Figure S4b. PXRD characterisation of powder of **6** zafirlukast:piperazine:toluene 3:3:2 cocrystal, performed as described in the methods section.

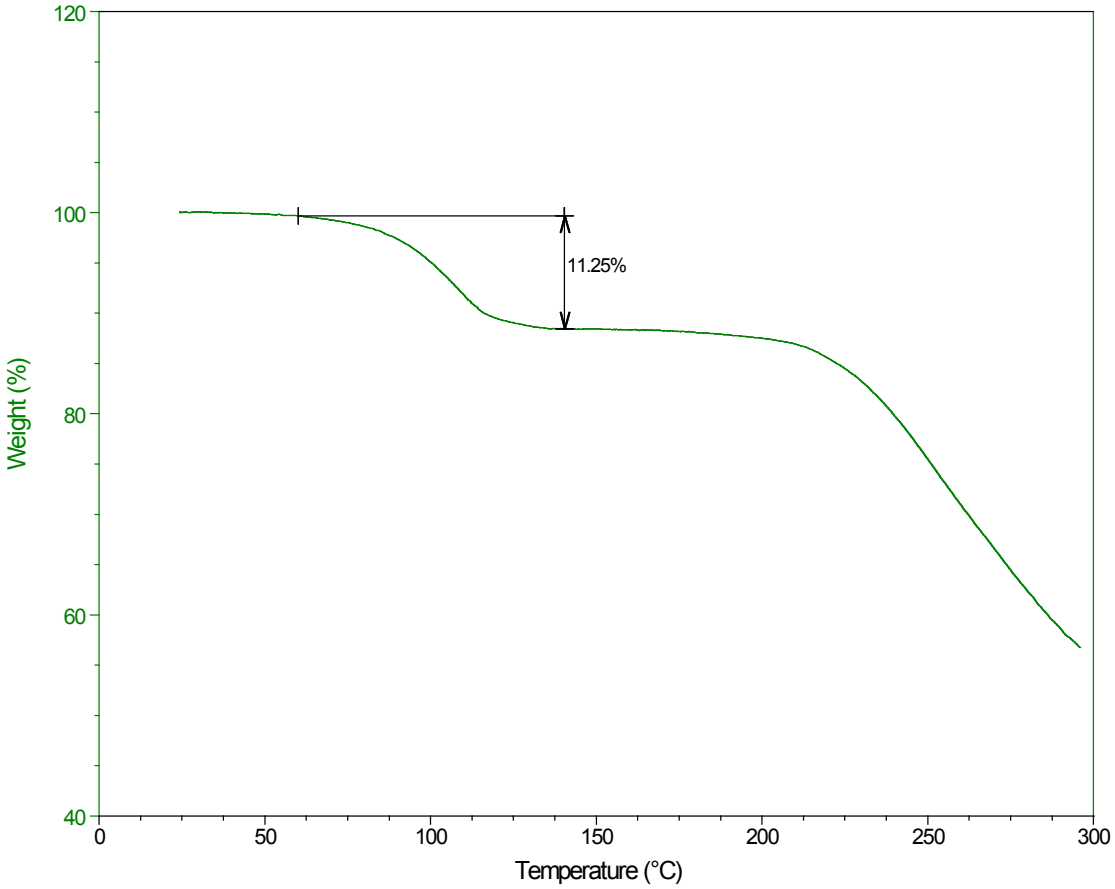

Figure S4c. TGA characterisation of powder of **6** zafirlukast:piperazine:toluene 3:3:2 cocrystal, performed as described in the methods section.

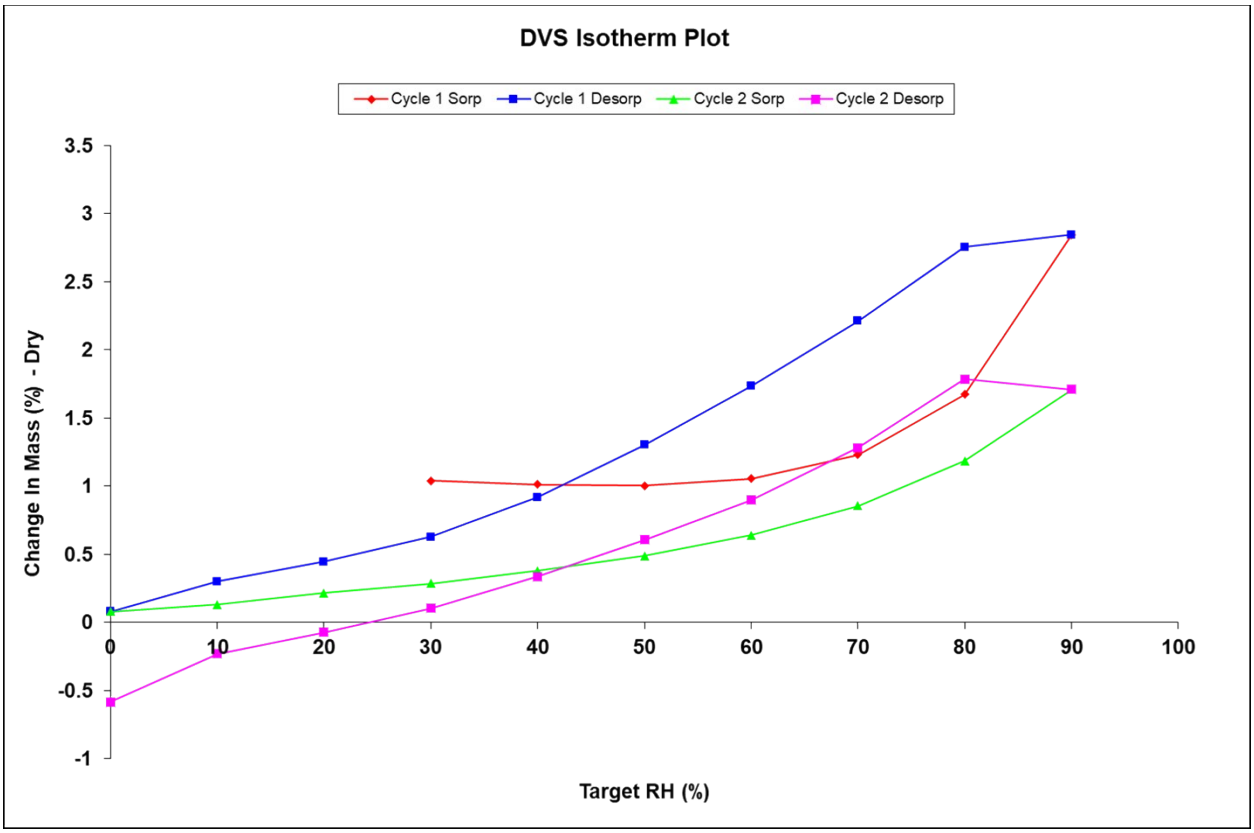

Figure S4d. DVS characterisation of powder of **6** zafirlukast:piperazine:toluene 3:3:2 cocrystal (isotherm plot), performed as described in the methods section.

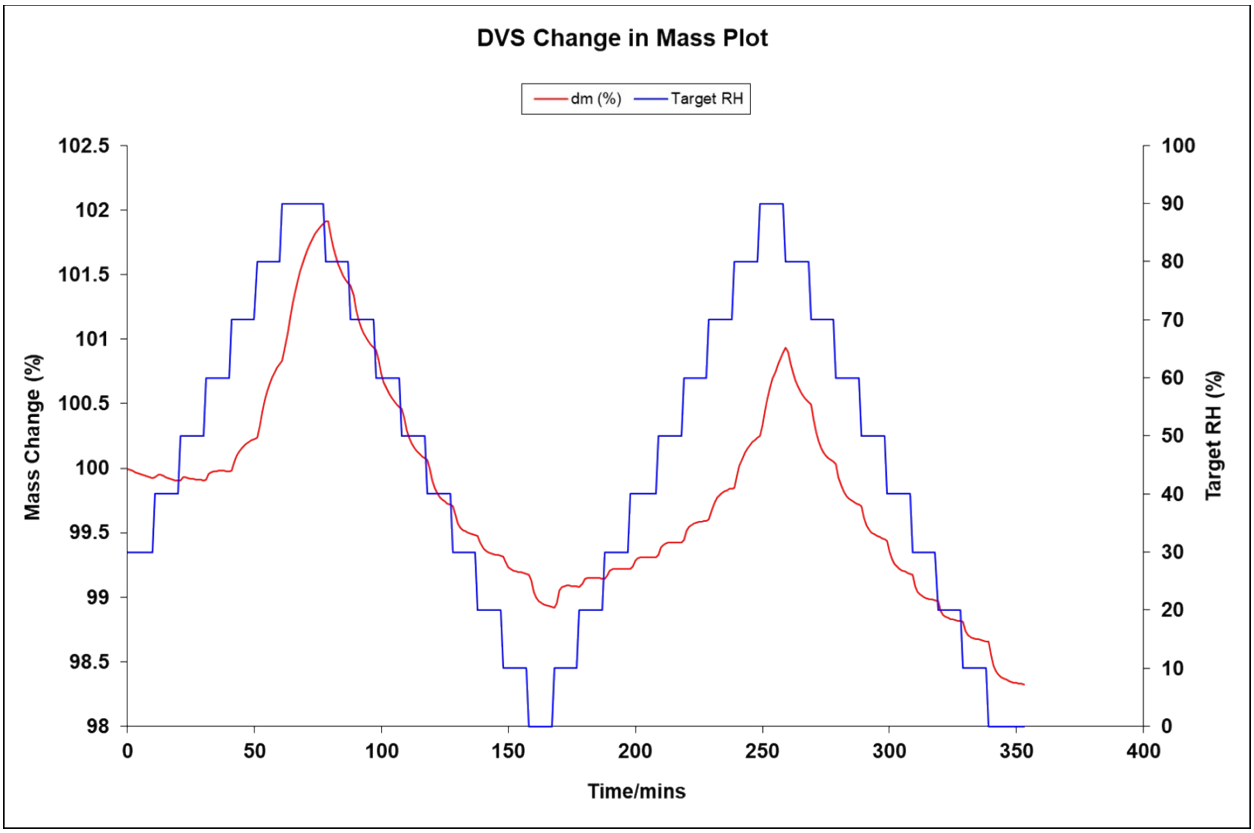

Figure S4e. DVS characterisation of powder of **6** zafirlukast:piperazine:toluene 3:3:2 cocrystal (change in mass plot), performed as described in the methods section.

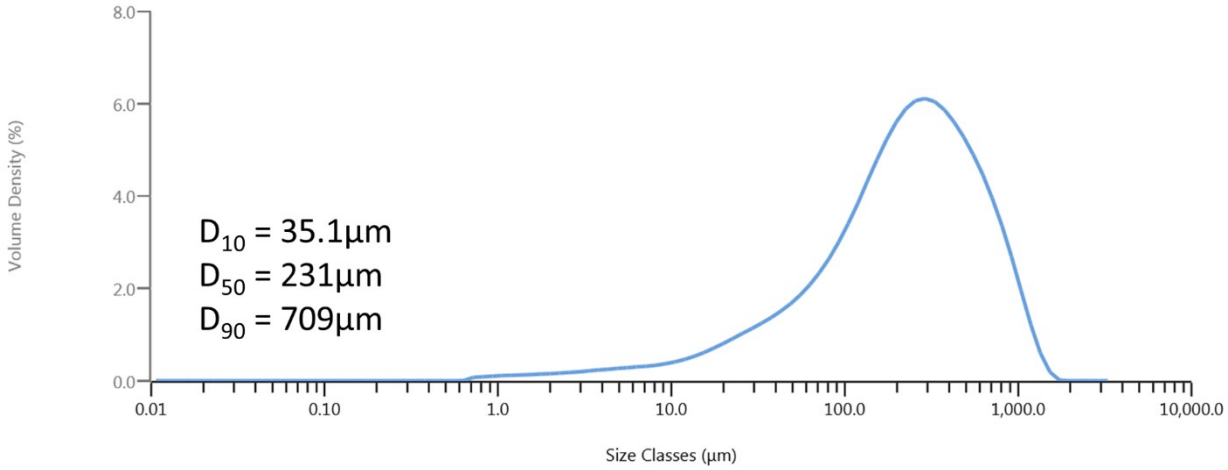

Figure S4f. Particle size determination of powder of **6** zafirlukast:piperazine:toluene 3:3:2 cocrystal, performed as described in the methods section.

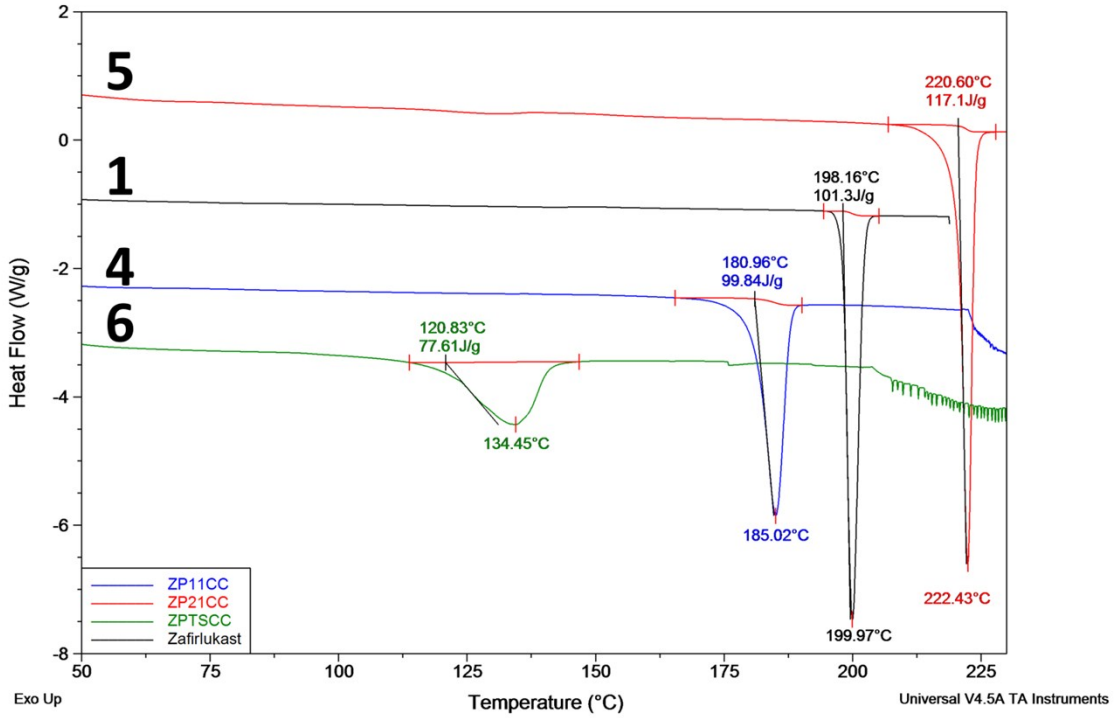

Figure S5. Comparison of DSC traces within the differing forms. Zafirlukast (**1**), Zafirlukast: piperazine 1:1 (**4**), Zafirlukast: piperazine 2:1 (**5**), Zafirlukast:piperazine:toluene 3:3:2 (**6**)

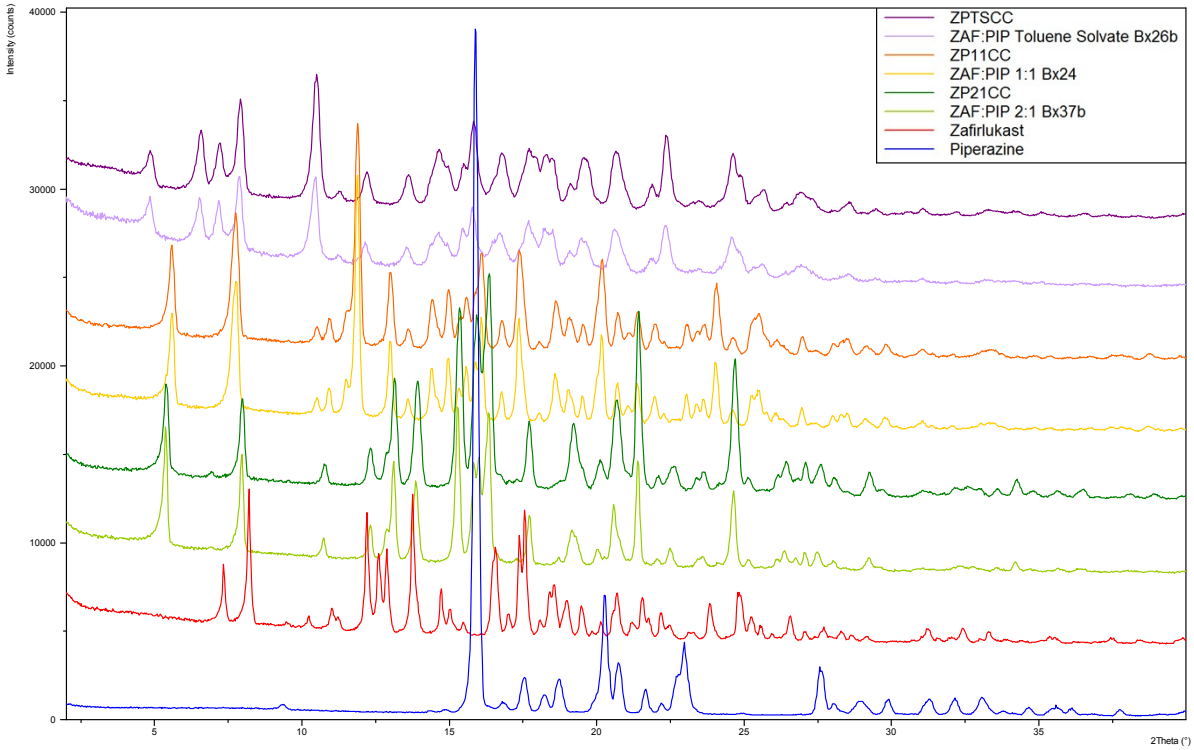

Figure S6. X-ray comparison witihin the differing forms.

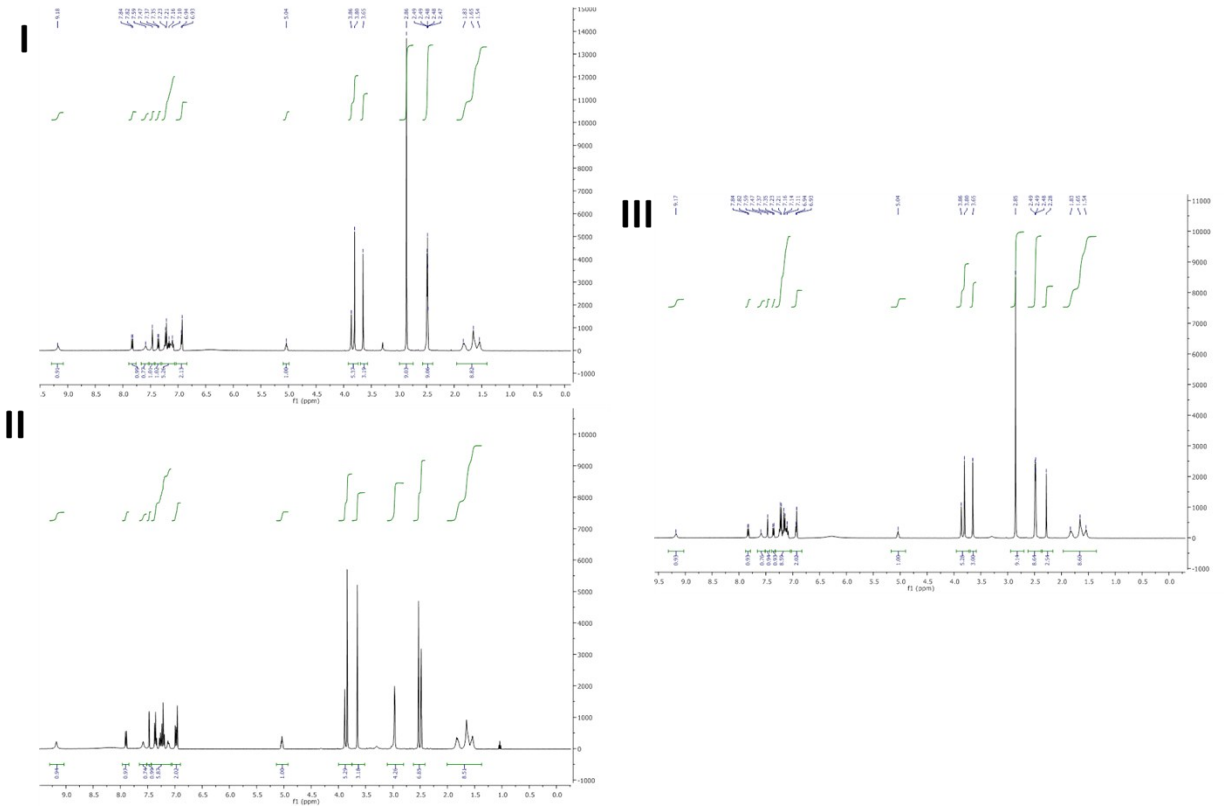

Figure S7. Comparison of ^{1}H-NMR (dmso-d_6) traces: I, **4** Zafirlukast:Piperazine cocrystal (1:1), II **5** Zafirlukast:Piperazine cocrystal (2:1), III **6** Zafirlukast:piperazine:toluene cocrystal (3:3:2).

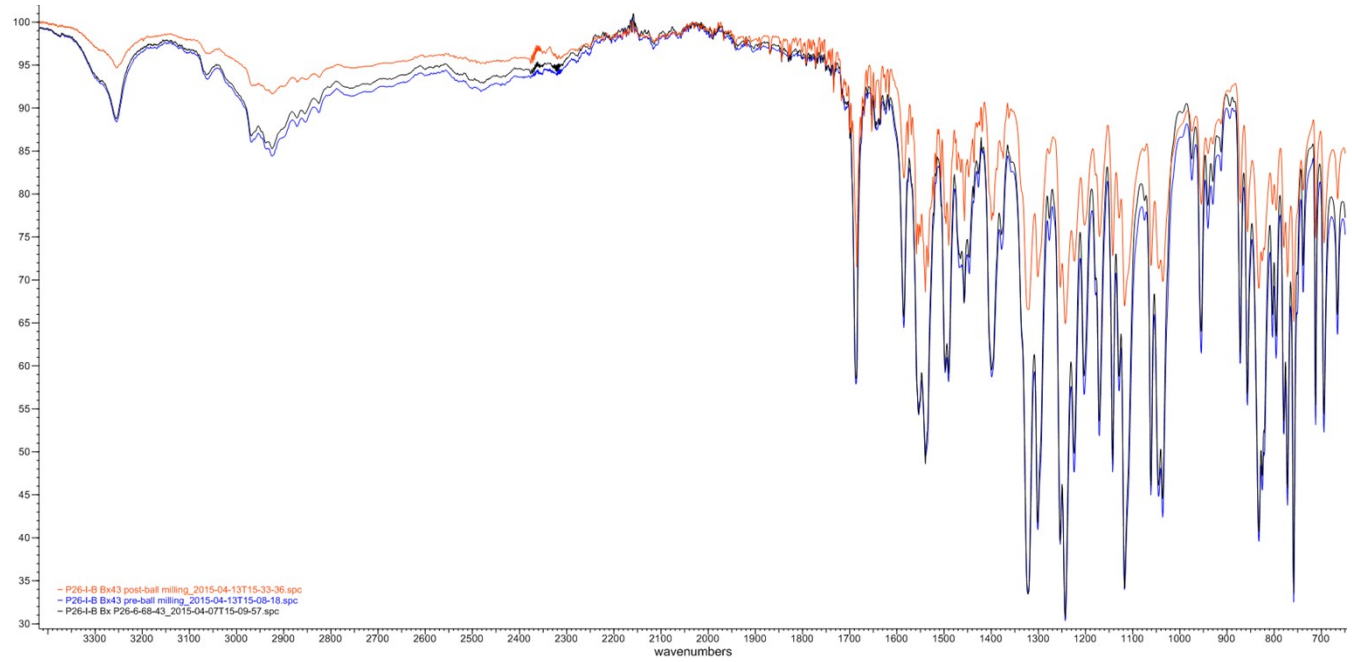

Figure S8. Comparison of differing batches and post ball milling by IR, showing no change in **4**

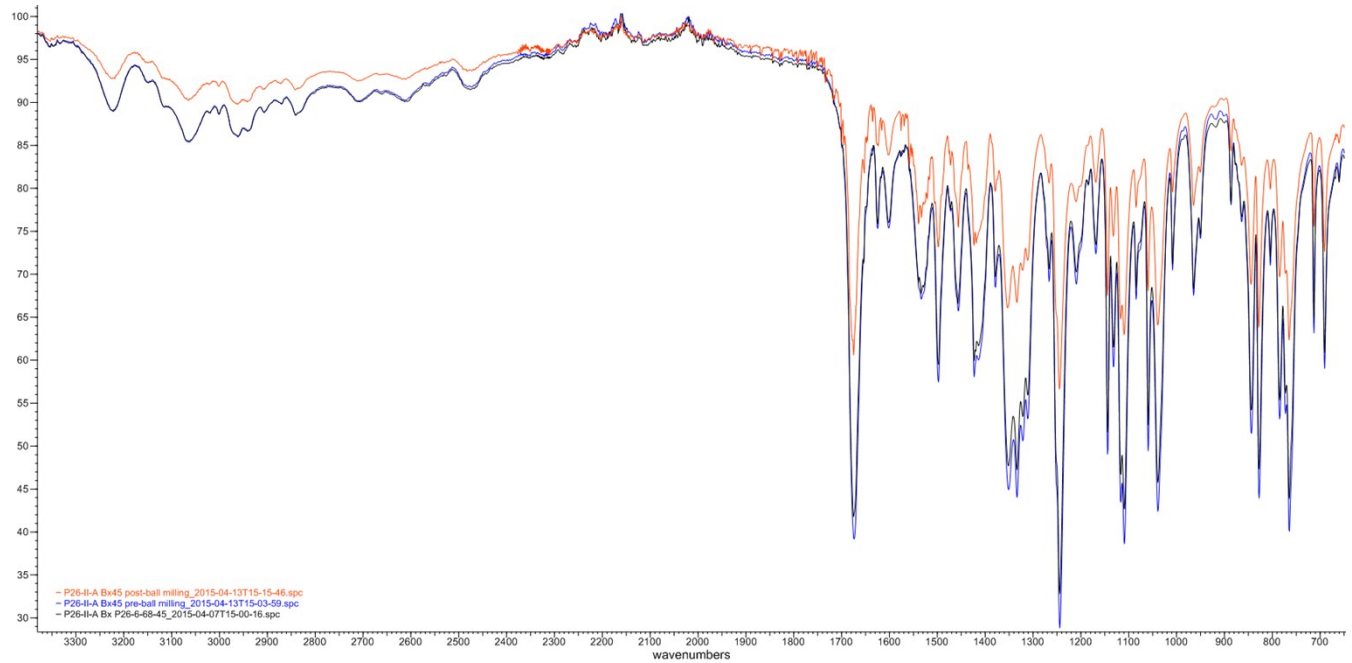

Figure S9. Comparison of differing batches and post ball milling by IR, showing no change in **5**

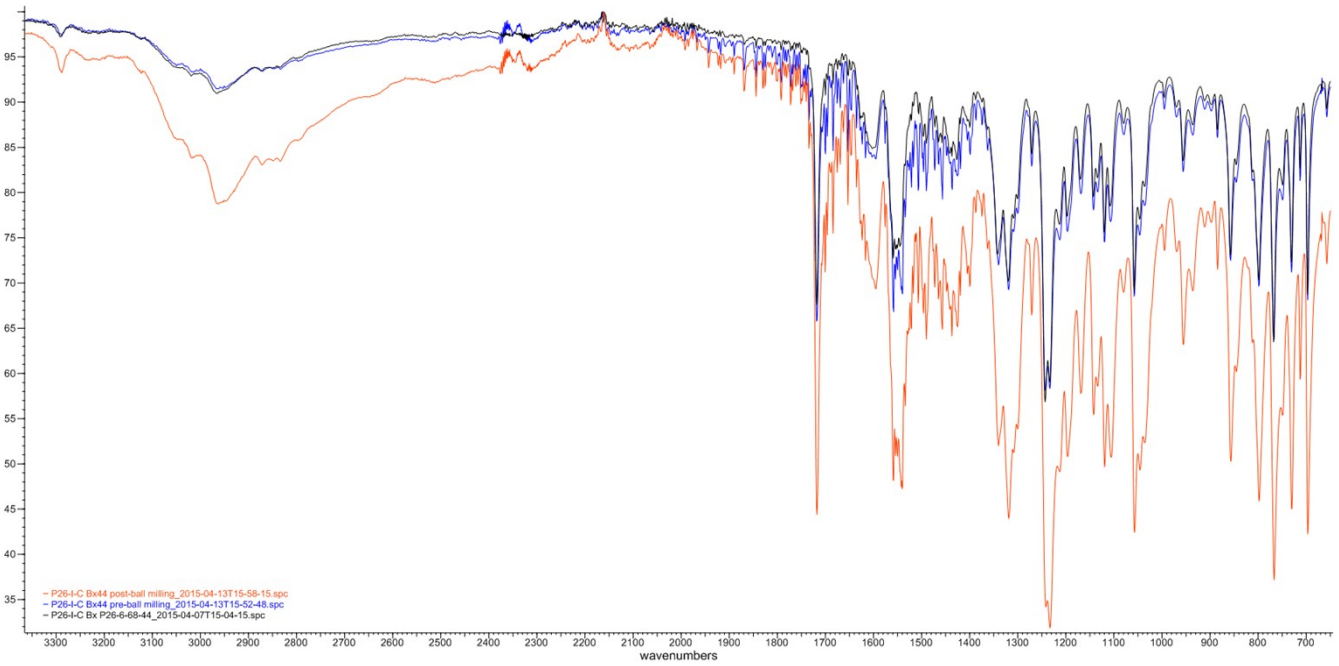

Figure S10. Comparison of differing batches and post ball milling by IR, showing changes in **6** which resulted in an inability to mill the form to a consistent particle size before formulation.

Calibration of HPLC method

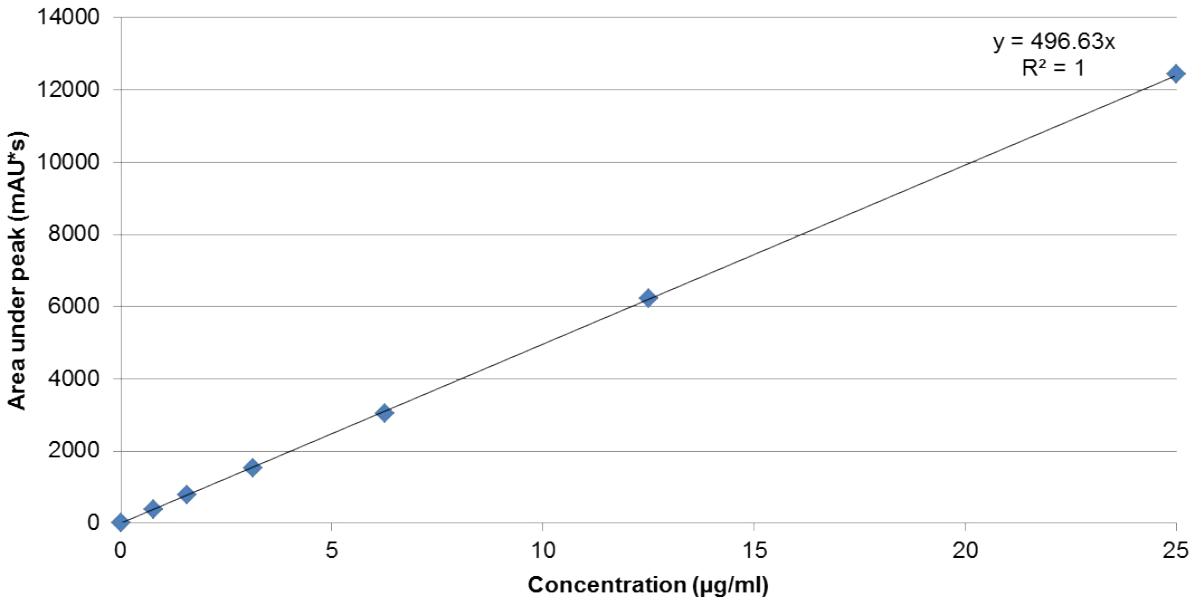

Figure S11. Calibration curve HPLC solubility analysis of zafirlukast.

Uniformity of content determination. For each of the four powder blends produced, three samples were taken for analysis. This was accomplished by first pouring the powder out of its container into a line on a sheet of clean paper. The three samples were taken approximately equidistantly along the line. The samples which were approximately 5-40 mg were weighed and the accurate mass recorded. To this 1.5 ml of solvent was added and sonication used to aid dissolution. A 1 in 100 dilution was performed and the resultant solution analysed by HPLC. The concentration of Zafirlukast of each sample solution was determined and compared to the calculated expected mass for each material taking into account the differences in stoichiometry. This was combined with a uniformity of mass calculation, to ensure the appropriate content was in each dosed capsule.

Table S12. Uniformity of content for *in vivo* dosing

Sample	Peak Area	Ret. Time	Diluted Conc. (µg/ml)	Conc. (µg/ml)	Mass of ZAF (mg)	Mass of Blend (mg)	Zaf content of blend	Calc. mass ZAF (mg)	ZAF content (as % of calculated)	Mean % of stated dose	SD
(**1**)/ 1	2352.55322	3.633	4.737034	473.70	0.7105	8.815	8.06%	0.8815	80.60%		
(**1**)/ 2	2576.80566	3.634	5.188582	518.85	0.7783	9.575	8.13%	0.9575	81.28%	**1**	
(**1**)/ 3	1296.34143	3.631	2.610276	261.027	0.3915	4.500	8.70%	0.4500	87.01%	82.96%	3.52%
(**4**)/ 1	2040.56372	3.634	4.108820	410.88	0.6163	7.390	8.34%	0.6427	95.90%		
(**4**)/ 2	2178.91699	3.629	4.387405	438.74	0.6581	8.920	7.38%	0.7758	84.84%	**4**	
(**4**)/ 3	3410.01172	3.631	6.866302	686.63	1.0230	12.785	8.06%	1.1119	92.63%	91.12%	5.68%
(**5**)/ 1	2620.77515	3.631	5.277118	527.71	0.7916	10.145	7.80%	0.9436	83.89%		
(**5**)/ 2	2461.79053	3.630	4.956991	495.69	0.7435	9.470	7.85%	0.8808	84.42%	**5**	
(**5**)/ 3	2451.16846	3.629	4.935602	493.56	0.7403	8.515	8.69%	0.7919	93.48%	87.27%	5.39%
(**6**)/ 1	860.81189	3.628	1.733306	173.33	0.2600	4.105	6.33%	0.3269	79.54%		
(**6**)/ 2	1635.43359	3.628	3.293062	329.31	0.4940	5.880	8.40%	0.4682	105.51%	**6**	
(**6**)/ 3	865.40167	3.630	1.742548	174.25	0.2614	3.570	7.32%	0.2843	91.95%	92.33%	12.98 %

These powders were then loaded into capsule which were analysed for their content in terms of stated mass.

Table S13. Uniformity of mass for *in vivo* dosing, ensuring that the appropriate known dose was delivered to the rats.

Compound	MW	mmoles	Weight (mg)	Powder blend				
				Mass used (mg)	Lactose needed	Lactose used	mg/mg	Need per cap.
Zafirlukast	575.68	0.002171	1.25	10.3572	93.2148	93.21	0.100004635	12.49942069
ZAF:PIP (1:1)	661.816	0.002171	1.436803	12.5595	113.0355	113.06	0.099980497	14.37080279
ZAF:PIP (2:1)	618.748	0.002171	1.343302	13.6268	122.6412	122.69	0.099964201	13.4378106
ZAF:PIP (Tol. Sol.)	723.236	0.002171	1.570145	7.8451	70.6059	70.58	0.100033025	15.69581643

API	Capsule	mass full cap	mass empty cap	blend used (mg)	API (mg)	% of stated dose
ZAF	1	22.45	9.9	12.55	1.255058165	100.405%
	2	23.71	11.31	12.4	1.24005747	99.205%
	3	23.4	10.95	12.45	1.245057702	99.605%
				av	1.246724446	99.738%
				sd	0.006236385	
1:1 CC	1	24.81	10.49	14.32	1.431720712	99.646%
	2	24.75	10.33	14.42	1.441718762	100.342%
	3	24.5	10.12	14.38	1.437719542	100.064%
				av	1.437053005	100.018%
				sd	0.004108808	
2:1 CC	1	24.28	10.94	13.34	1.333522442	99.272%
	2	23.84	10.26	13.58	1.35751385	101.058%
	3	24.02	10.41	13.61	1.360512776	101.281%
				av	1.350516356	100.537%
				sd	0.01207872	
Tol. Sol.	1	26.24	10.35	15.89	1.589524769	101.237%
	2	26.21	10.62	15.59	1.559514862	99.326%
	3	26.19	10.32	15.87	1.587524109	101.110%
				av	1.57885458	100.558%
				sd	0.013699615	

Pharmacokinetics in individual rats

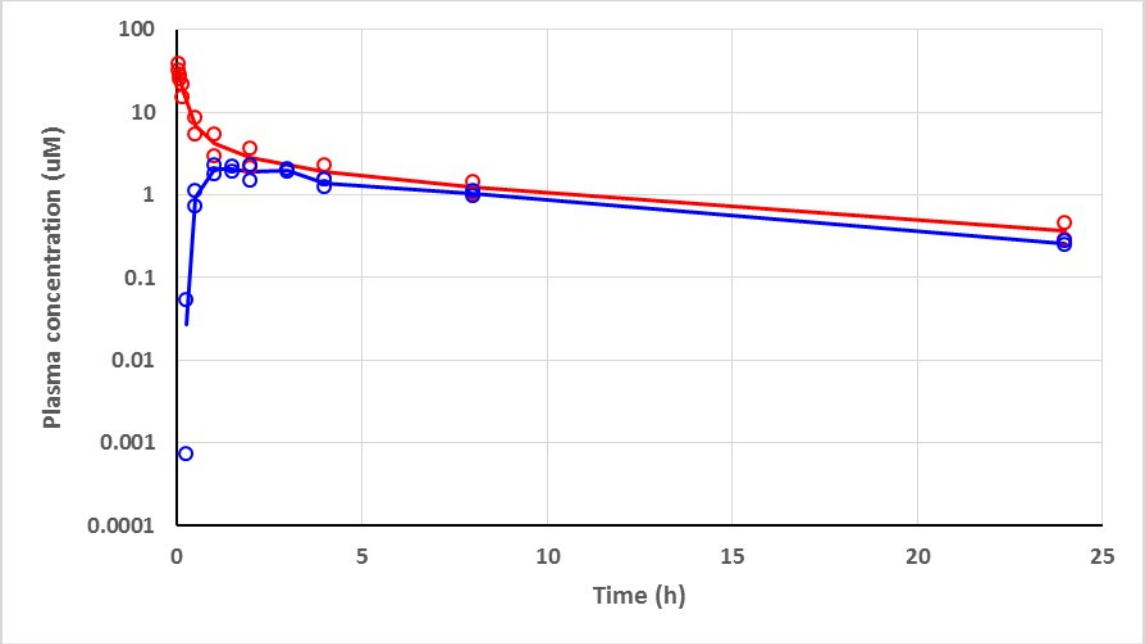

Figure S14. Pharmacokinetics of **1** in rat HW male (Dose IV 1 mg/Kg, dose oral capsule 5 mg/Kg)

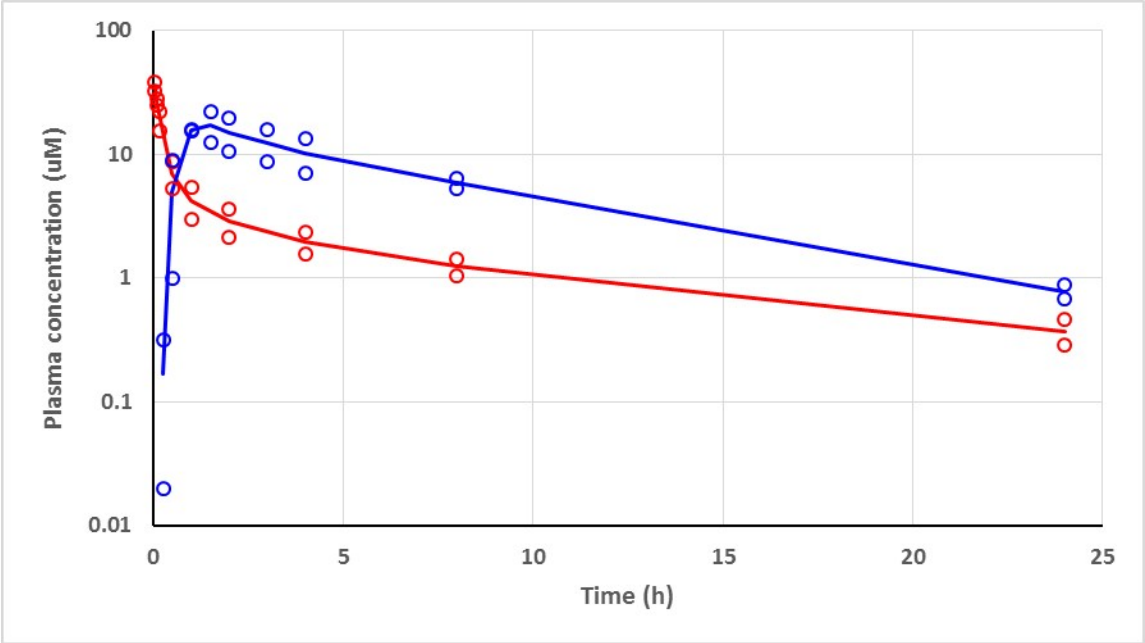

Figure S15. Pharmacokinetics of **4** in rat HW male (Dose IV 1 mg/Kg, dose oral capsule 5 mg/Kg)

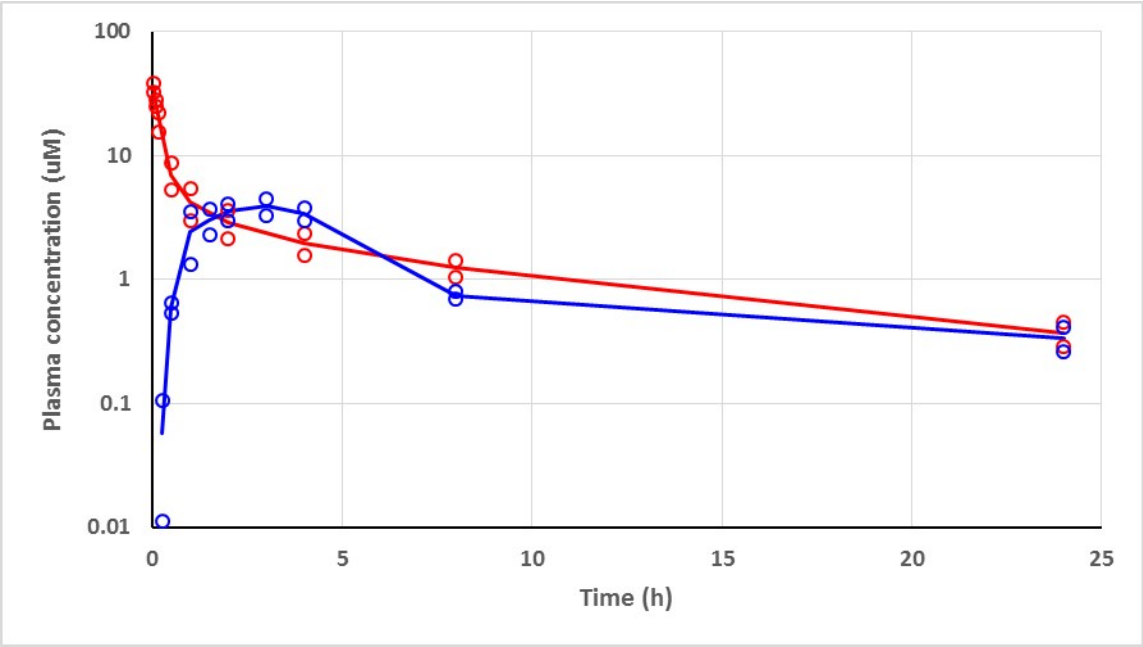

Figure S16. Pharmacokinetics of **5** in rat HW male (Dose IV 1 mg/Kg, dose oral capsule 5 mg/Kg)

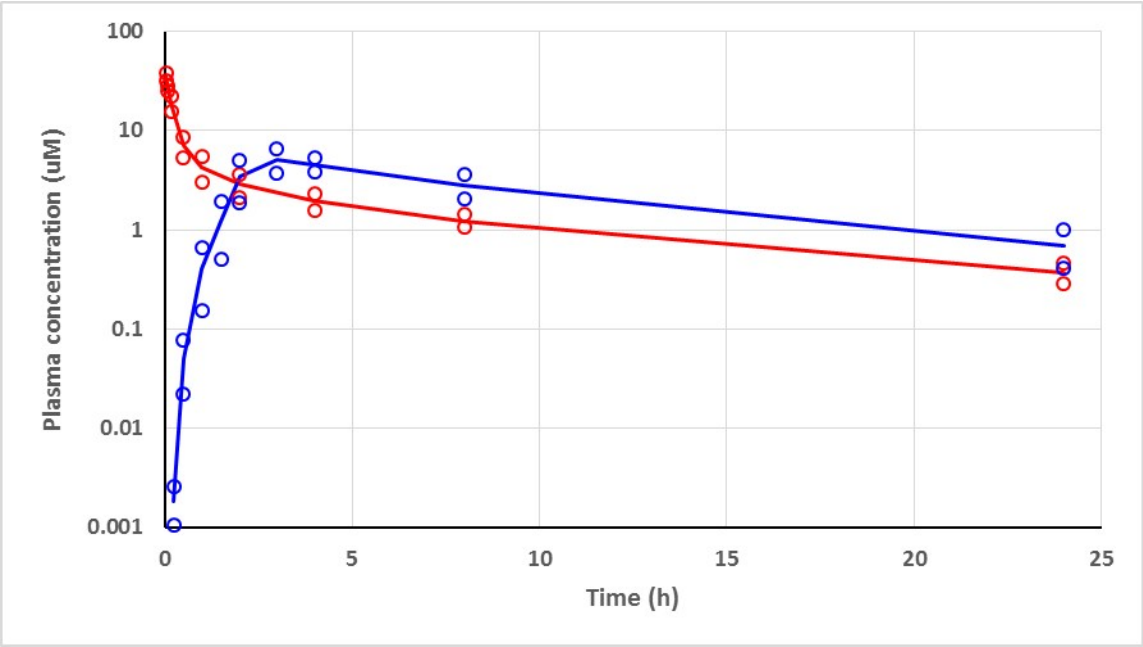

Figure S17. Pharmacokinetics of **6** in rat HW male (Dose IV 1 mg/Kg, dose oral capsule 5 mg/Kg)

Characterisation methods for produced batches

X-ray Powder Diffraction (XRPD) patterns were recorded for the produced cocrystals and compared to those of the reference patterns of the cocrystals to confirm equivalence. XRPD patterns were recorded on a PANalytical Empyrean diffractometer using Cu Kα radiation (λ = 1.54 Å), tube voltage of 40 kV and 40 mA current. Intensities were measured from 2° to 40° 2θ with 0.04 rad. Soller silts and an incident beam divergent slit of 1/8°, anti-scatter slit of 1/4° and diffracted beam anti-scatter slit of 7.5mm (PIXcel).

Differential Scanning Calorimetry (DSC) thermograms were recorded on a TA Q2000 using standard aluminium pans. Standard mode was used throughout and where heat/cool/heat cycles were used the initial heating phase was at a rate of 10°C/min, cooling cycle at 50°C/min and the second heating cycle at 10°C/min.

Infrared (IR) Spectroscopy FTIR spectra of solid phases were collected on either an Agilent Cary 630 FTIR spectrometer with diamond attenuated total reflectance (ATR) crystal accessory and 128 scans for each sample were collected at a resolution of 2 cm^{-1} over a wavenumber region of 4000-650 cm^{-1}; or a PerkinElmer Spectrum Two FTIR spectrometer with diamond universal ATR accessory and 4 scans for each sample were collected at a resolution of 2 cm^{-1} over a wavenumber region of 4000-600 cm^{-1}.

Dynamic Vapour Sorption (DVS) analysis was undertaken using a Surface Measurement Systems (London UK) DVS-1 with a 10% RH step between humidity values with equilibrium achieved at 0.1% weight change before moving to the next step. Methods were started at the humidity of the room at ambient (measured by a Rotronic A/H hygrometer) with subsequent

increase to 90%RH before cycling to 0%RH, to 90%RH, to 0%RH. Sample weights of between 5-20mg were used for all samples.

Thermogravimetric Analysis (TGA) profiles were recorded on a TA Q500 using standard platinum pans. The method used was a ramp at a rate of 10°C/min to 300°C maximum.

Proton Nuclear Magnetic Resonance (^{1}HNMR) spectra have been recorded on a Varian Mercury 400 (400 MHz). Chemical shifts for proton are reported in parts per million (ppm) downfield from tetramethylsilane and are referenced to residual protium in the NMR solvent (DMSO: D6 2.50).

High-Performance Liquid Chromatography (HPLC) analyses were performed using an Agilent 1260 Infinity fitted with an Agilent Eclipse Plus C18 reverse-phase column (3.5 µm particle size, 4.6 x 100 mm). The mobile phase used was a 30:70 ratio solution of pH 3.5 0.01 M KH2PO4 buffer and acetonitrile. Injection volume was 100 µl and elution of the sample constituents occurred over 6 minutes at a flow rate of 1 ml/min, with column temperature set at 22-25°C. The detector used was an Agilent 1260 VWD spectrophotometer set at a wavelength of 223 nm.

Particle size distribution A Mastersizer 3000 was used with the dry dispersion AeroS stage. A pressure of 4 bar was used with the micro-sample plate used for powder delivery. Where limited material was available post milling, particle size selection for formulation into capsules was achieved by sieving using Endocotts sieves of 75 and 38 µm.